THE TREFOIL: AN ANALYSIS IN CURVE MINIMIZATION AND SPLINE THEORY

by

TROY ARTHUR CLARK

Submitted in partial fulfillment of the requirements for the degree of

Doctor of Philosophy

Department of Mathematics, Applied Mathematics and Statistics

CASE WESTERN RESERVE UNIVERSITY

August 2020

CASE WESTERN RESERVE UNIVERSITY

SCHOOL OF GRADUATE STUDIES

We hereby approve the dissertation of

Troy Arthur Clark

Candidate for the degree of Doctor of Philosophy*

Committee Chair: ______________________________

Dr. David A. Singer
Dissertation Advisor
Professor, Department of Mathematics, Applied Mathematics and Statistics

Committee: ______________________________

Dr. Joel C. Langer
Professor, Department of Mathematics, Applied Mathematics and Statistics

Committee: ______________________________

Dr. Elisabeth M. Werner
Professor, Department of Mathematics, Applied Mathematics and Statistics

Committee: ______________________________

Dr. Colin S. McLarty
Truman P. Handy Professor of Philosophy, Department of Philosophy

Date of Defense: July 31, 2020

*We also certify that written approval has been obtained for any proprietary material contained therein.

CONTENTS

LIST OF FIGURES

LIST OF TABLES

ACKNOWLEDGMENTS

I would like to express my deepest gratitude to my research advisor, Dr. David Singer. While I may be very difficult to work with, he was patient and supportive in my development towards my academic progress. Thank you for boosting my confidence when I did not pass the qualifying exam on my first attempt and thank you for building up my abstract algebra skills so I would be ready for the second time around. Thank you for helping me realize that failure is a part of success and that epiphanies will come when they may. I could not have asked for a better advisor and I hope to become as great of a person as he is. I would like to deeply thank the members of my dissertation committee: Dr. Joel Langer (my "co-advisor"), Dr. Elisabeth Werner and Dr. Colin McLarty. Thank you for the knowledge you shared with me in the courses that I had with you all. Your expertise and your enthusiasm for your respective fields made me thirst to understand more about a subject that I grew to love and appreciate.

I would like to thank all the teachers, instructors and professors that I've had over the years. Thank you for inspiring me to become the mathematician that I am today and thank you for never giving up on me when I struggled. Thank you to all the classmates that I had over the years. Honestly, without you all, I would've dropped out of graduate school a long time ago. Thank you for helping me through the difficult times and realizing my potential.

I could not have done this without the help of the administrative staff of Case Western Reserve University during the time I was there. Thank you for taking the time to answer questions, refer me to the proper people and making sure I had the correct forms. A big special thank you to a former member of the administrative staff, Katie Gaffen. If I had never received your phone call, I would have never knew that I was accepted to the doctoral program at Case, due to the acceptance letter being lost in the mail. To be honest, none of this would be possible without you.

A special thanks to Cuyahoga Community College and the tutoring center for allowing me to influence and inspire students to appreciate the beautiful subject of mathematics for over six years. My fellow co-workers always encouraged me and I always felt accepted and respected by them. My deepest gratitude to the students I've encountered over the years. Because of all of you, I've became a better teacher, a more patient person and an efficient problem solver.

On a personal note, I wish to thank my mother (Mary), my sister (Traci) and my nephew (Chance) for all of their love and support throughout the years. We may be a small family but I could not ask for a better one. I want to express a special thanks to Veronica Beckstrom and her family for their love, unwavering support and for understanding the trials of being a graduate student. The fact you provided me with food, supplies and everything else I needed to get through the last few months means the world to me. Thank you for being patient and understanding.

A Bette Midler song once stated: "You got to have friends." I truly could not have made it through graduate school (and life) without the many friends I made along the journey. I want to extend a special thank you to my friends over the years (inside and outside academia). Thank you for sticking by me even when there were times I was too tired to go out, canceled at the last minute or could not afford to hang out. To my academia friends, I always value our conversations, misadventures, teatime and various activities we did together. We could not have made it through graduate school alone and I am so happy that we have met. To my friends, thank you for giving me a reason to smile when I wanted to cry.

Lastly, there are five people who are not longer with us that I wish to acknowledge: Kristine Gehrs, Linda Mastrodonato, Dr. J. Michael Harding, Louraine Collins and Douglas Scholle. Thank you for all your lessons, confidence and faith in me. I'm happy that our paths crossed in life and you all will never be forgotten.

The Trefoil: An Analysis in Curve Minimization and Spline Theory

Abstract

by

TROY ARTHUR CLARK

We will consider a variational problem arising out of the localized induction equation. We are motivated by the idea of finding "fair" splines, by considering an energy functional involving the derivative of the curvature. Among the solutions to the Euler-Lagrange equations are two elastic curves and the Kiepert Trefoil. We will introduce features and properties of the trefoil. One of the features of the trefoil is that it is an algebraic curve with a simple parametrization to handle. In addition to this, we will show that the trefoil is a model for a two-parameter spline and provide examples of how pieces of the trefoil can be cut, transformed and fitted so that the resulting curve is aesthetically "fair".

Introduction

What is the goal of this thesis? Well, we are studying a family of curves defined by a variational problem arising from the Localized Induction Equation. Among the solutions to the problem, two special ones are elastic curves. The third is the Kiepert trefoil, which has a number of remarkable properties. The trefoil is a model of a two parameter family of splines. We will show that it satisfies the conditions to be such a model and explore its properties.

In Chapter 1, we will provide a brief introduction to the calculus of variations. We will need to understand the theory behind the subject due to its use to find variational solutions to our problem. We will look at the derivations of the Euler-Lagrange and the Euler-Poisson equations, both key in finding solutions that extremize functionals. It is in this chapter where we will propose a new energy functional where its solutions would be considered as good candidates for splines. One of these solutions is the Kiepert trefoil. Further work in this claim will be explored in Chapter 5.

Chapter 2 will discuss exactly what an elliptic function is and some of their properties. We will also discuss different types of elliptic function: Weierstrass, Jacobi and Dixon since our solutions will be in terms of these functions. Further calculations of these functions will be provided in Chapter 5.

Chapter 3 will discuss splines. It is here where the notion of "fairness" will be discussed and different variations of the definition. We will also cover some desirable properties that we wish for splines to satisfy, such as roundness, extensionality and locality. Levien's criterion for a curve to be a model for a two-parameter family of splines will be introduced, along with a more geometric proof for general curves.

Chapter 4 gives a small history of the Minimum Energy Curve, the Euler elastica and the derivation of its solutions via calculus of variations and differential geometry. These derivations will be needed in the next chapter when we derive the Euler-Lagrange equation for our proposed functional. The chapter ends with a discussion about the Minimum Variation Curve, defined as the integral of the squared change of curvature. We will discuss some properties this functional holds and why is it a better metric than the Minimum Energy Curve.

Chapter 5 is the heart of this thesis, where we analyze the special solutions of our proposed metric for desirable candidates for splines. We will primarily focus on the Kiepert trefoil and its properties. We will also explore scale-invariant minimizations of our special solutions along with proposed analytical/numerical solutions based on the behaviors of elliptic functions.

In Chapter 6, we will start with observing a special value that came from the criterion mentioned in Chapter 3. This value is called the aberrancy and has a special geometric relationship to curves. We will show that the three solutions to our proposed metric satisfy the criterion mentioned in Chapter 4. In addition to this, we will also provide examples of how the trefoil produces a suitable spline for circumscribed circles around a regular polygon and a few special cases with general polygons.

In Chapter 7, we will close out the thesis with some numerical computations of the trefoil spline via Mathematica. These numerical solutions will provide us a way to find certain measures of angles in our spline given a set of predetermined values. We will also present a number of non-circular examples of how the trefoil can be used in splines, primarily in fonts.

Chapter 1

Calculus of Variations

1.1 An Introduction

The formation of calculus of variations came almost simultaneously with that of differential and integral calculus. While it can be argued that the first person to solve a problem of calculus of variations was Queen Dido of Carthage, it is undisputed that Sir Issac Newton was the first mathematician to publish a result in this field [61]. In 1696, Johann Bernoulli furthered the development by publishing a letter in which he advanced the problem of the line of quickest descent, the brachistochrone problem. In 1698, Jacob Bernoulli solved the problem involving geodesics, which determined the line of minimum length that connects two points on a surface. However, a more general solution would later be formulated by both Leonhard Euler and Joseph-Louis Lagrange [21], [26]. Calculus of variations was just a mathematical curiosity and it was not until the works of Leonhard Euler that it became its own independent mathematical discipline. One of Euler's contributions was his general solution to the isoperimetric problem, which asks to find a closed curve of a given length such that it bounds a maximum area. Due to his own extensive work in the subject, some may even consider Euler to be the founder of calculus of variations. In 1760, Joseph-Louis Lagrange introduced a general method of dealing with variational problems connected to mechanics [41].

In differential calculus, if given a function $f(x)$, we find the extrema by taking the derivative $f'(x)$ and set it equal to 0. The values of x where $f'(x) = 0$ tell us where the slope of the curve is constant, hence why these values are called *stationary points*. However, we would have to do further testing to see whether these points qualify as maxima, minima or neither. This is usually done by the utilization of the *Second Derivative Test*.

The goal of calculus of variations is to systematize the theory of the extrema of functions of a finite number of independent variables [41]. Here, we deal with *functionals*, which are maps from a space of functions (which can be continuous, smooth, etc.) to $\mathbb{R}$ or $\mathbb{C}$. Instead of finding stationary points, we will need to find stationary functions, which will involve differential equations. For the purpose of calculus of variations, the functionals $F[y]$ are generally written as integrals in the form

$$F[y] = \int_{x_0}^{x_1} f(x, y(x), y'(x))dx.$$

We wish to find the extrema of this function which satisfies the boundary conditions of

$$y(x_0) = y_0 \qquad y(x_1) = y_1.$$

Numerous laws and problems of mechanics and physics can be reduced to the statement that a certain functional in a given process has to reach a maximum or minimum. Such laws and problems are called *variational*. Some variational principles or consequences of them include the principle of least action, the law of the conservation of energy, the law of the conservation of motion, amongst others [26].

1.2 The Euler-Langrange Equation

Consider the variational problem

$$F[y] = \int_{x_0}^{x_1} f(x, y(x), y'(x))\, dx,$$

where the solution satisfies the boundary conditions

$$y(x_0) = y_0 \qquad y(x_1) = y_1.$$

Suppose there is a solution $y(x)$ for the problem above which satisfies the boundary conditions and produces the functional's extremum. We will also assume that $y(x)$ is twice differentiable. To show that this function produces an extremum, we will need to show that any alternative must fail [46].

Consider a family of admissible functions:

$$Y(x) = y(x) + \epsilon\eta(x),$$

where $\eta(x)$ is an arbitrary fixed function of x, that is also twice-differentiable and vanishes at both endpoints

$$\eta(x_0) = \eta(x_1) = 0.$$

This ensures us that $Y(x_0) = y_0$ and $Y(x_1) = y_1$.

Now since $Y(x)$ satisfies the boundary conditions, we can substitute $Y(x)$ for $y(x)$ in the functional

$$F[\epsilon] = \int_{x_0}^{x_1} f(x, Y(x), Y'(x))\, dx,$$

where $Y'(x) = y'(x) + \epsilon\eta'(x)$.

The new functional is identical to the original when $\epsilon = 0$ and reaches its extremum when

$$\left.\frac{\partial F[\epsilon]}{\partial \epsilon}\right|_{\epsilon=0} = 0.$$

Performing the derivation and taking the resulting derivative into the integral (the limits of integration are fixed) with the chain rule results

$$\frac{\partial F[\epsilon]}{\partial \epsilon} = \int_{x_0}^{x_1} \left(\frac{\partial F}{\partial Y}\frac{dY}{d\epsilon} + \frac{\partial F}{\partial Y'}\frac{dY'}{d\epsilon}\right) dx.$$

Now clearly,

$$\frac{dY}{d\epsilon} = \eta(x) \quad \text{and} \quad \frac{dY'}{d\epsilon} = \eta'(x),$$

which results in

$$\frac{\partial F[\epsilon]}{\partial \epsilon} = \int_{x_0}^{x_1} \left(\frac{\partial F}{\partial Y}\eta(x) + \frac{\partial F}{\partial Y'}\eta'(x)\right) dx.$$

Integrating the second terms by parts yields

$$\int_{x_0}^{x_1} \Big(\frac{\partial F}{\partial Y'}\eta'(x)\Big)\ dx = \frac{\partial F}{\partial Y'}\eta(x)\Big|_{x_0}^{x_1} - \int_{x_0}^{x_1} \Big(\frac{d}{dx}\frac{\partial F}{\partial Y'}\Big)\eta(x)\ dx$$
$$= 0 - \int_{x_0}^{x_1} \Big(\frac{d}{dx}\frac{\partial F}{\partial Y'}\Big)\eta(x)\ dx$$
$$= - \int_{x_0}^{x_1} \Big(\frac{d}{dx}\frac{\partial F}{\partial Y'}\Big)\eta(x)\ dx$$

By substitution, the problem becomes

$$\frac{\partial F[\epsilon]}{\partial \epsilon} = \int_{x_0}^{x_1} \Big(\frac{\partial F}{\partial Y} - \frac{d}{dx}\frac{\partial F}{\partial Y'}\Big)\eta(x)\ dx.$$

The extremum is achieved when $\epsilon = 0$, thus

$$\frac{\partial F[\epsilon]}{\partial \epsilon}\Big|_{\epsilon=0} = \int_{x_0}^{x_1} \Big(\frac{\partial F}{\partial y} - \frac{d}{dx}\frac{\partial F}{\partial y'}\Big)\eta(x)\ dx.$$

Now, we need to state a lemma:

Lemma 1.2.1 *(The Fundamental Lemma of the Calculus of Variations) Suppose that $G(x)$ is continuous and $\eta(x)$ is continuously differentiable over the interval [x_0,x_1] such that $\eta(x_0) = \eta(x_1) = 0$. Then if for all such $\eta(x)$,*

$$\int_{x_0}^{x_1} \eta(x)G(x)\ dx = 0,$$

then

$$G(x) = 0$$

in the whole interval.

Proof . By means of contradiction, assume that there exists at least one such value ζ where $x_0 \le \zeta \le x_1$ such that $G(x)$ is not zero. Without loss of generality, suppose $G(\zeta) > 0$. Then by the condition of continuity of $G(x)$, there must be a neighborhood $\zeta - h \le \zeta \le \zeta + h$ where $G(x) > 0$. However, the integral becomes

$$\int_{x_0}^{x_1} \eta(x) G(x)\, dx > 0,$$

for the right choice of $\eta(x)$, which forms our contradiction. Hence, the statement of the lemma must be true. ∎

By applying the lemma to the work above, we arrive at the *Euler-Lagrange Equation*

$$\frac{\partial F}{\partial y} - \frac{d}{dx}\frac{\partial F}{\partial y'} = 0,$$

which gives us a necessary and sufficient condition for $y(x)$ to be a stationary function of $F[y]$ [46]. The Euler-Lagrange Equation can be generalized for functionals containing higher derivatives or multiple functions. One such generalization for when higher derivatives are involved, the *Euler-Poisson equation*, will be discussed and derived in the next section. Believe it or not, the derivation of these equations is actually the *easiest* part of the calculus of variations. The hardest part is actually solving these equations, which will involve differential equations. These differential equations may be of higher order and may or may not even be linear!

1.3 The Euler-Poisson Equation

The Euler-Lagrange equation will not be enough to solve general variational problems since it can only handle functionals written in terms of the first derivative. For this, we will need to define a more general version of the Euler-Lagrange equation called the *Euler-Poisson equation*.

Suppose we have a variational problem with a functional that has a single function but instead of having a first derivative, it has higher order ones

$$J[y] = \int_{x_0}^{x_1} f(x, y, y', ..., y^{(m)})\ dx.$$

In addition, we are given the following boundary conditions

$$\begin{gathered} y(x_0) = y_0, \quad y(x_1) = y_1 \\ y'(x_0) = y_0', \quad y'(x_1) = y_1' \\ y''(x_0) = y_0'', \quad y''(x_1) = y_1'' \\ \vdots \\ y^{(m-1)}(x_0) = y_0^{(m-1)}, \quad y^{(m-1)}(x_1) = y_1^{(m-1)} \end{gathered}$$

As noted in the first chapter, consider a family of admissible functions:

$$Y(x) = y(x) + \epsilon\eta(x),$$

where $\eta(x)$ is an arbitrary fixed function of x, that is continuously differentiable and vanishes at both endpoints

$$\eta(x_0) = \eta(x_1) = 0,$$

as does its derivative

$$\eta'(x_0) = \eta'(x_1) = 0.$$

The variational problem in terms of this set of functions is:

$$J[\epsilon] = \int_{x_0}^{x_1} f(x, Y, Y', ..., Y^{(m)})\; dx$$

Taking the derivative with respect to ϵ gives

$$\frac{dJ}{d\epsilon} = \int_{x_0}^{x_1} \frac{d}{d\epsilon} f(x, Y, Y', ..., Y^{(m)})\; dx$$

and by using the chain rule, we can rewrite the integrand as

$$\frac{\partial f}{\partial Y}\frac{dY}{d\epsilon} + \frac{\partial f}{\partial Y'}\frac{dY'}{d\epsilon} + \frac{\partial f}{\partial Y''}\frac{dY''}{d\epsilon} + \cdots + \frac{\partial f}{\partial Y^{(m)}}\frac{dY^{(m)}}{d\epsilon}.$$

Now by substituting Y and its derivatives with respect to ϵ yields

$$\frac{\partial f}{\partial Y}\eta + \frac{\partial f}{\partial Y'}\eta' + \frac{\partial f}{\partial Y''}\eta'' + \cdots + \frac{\partial f}{\partial Y^{(m)}}\eta^{(m)}.$$

The function then becomes

$$\frac{dJ}{d\epsilon} = \int_{x_0}^{x_1} \Big(\frac{\partial f}{\partial Y}\eta + \frac{\partial f}{\partial Y'}\eta' + \frac{\partial f}{\partial Y''}\eta'' + \cdots + \frac{\partial f}{\partial Y^{(m)}}\eta^{(m)}\Big)\; dx.$$

Integrating by terms produces

$$\frac{dJ}{d\epsilon} = \int_{x_0}^{x_1} \frac{\partial f}{\partial Y}\eta\; dx + \int_{x_0}^{x_1} \frac{\partial f}{\partial Y'}\eta'\; dx + \int_{x_0}^{x_1} \frac{\partial f}{\partial Y''}\eta''\; dx + \cdots + \int_{x_0}^{x_1} \frac{\partial f}{\partial Y^{(m)}}\eta^{(m)}\; dx$$

and integrating by parts gives

$$\frac{dJ}{d\epsilon} = \int_{x_0}^{x_1} \eta\frac{\partial f}{\partial Y}\; dx - \int_{x_0}^{x_1} \eta\frac{d}{dx}\frac{\partial f}{\partial Y'}\; dx + \int_{x_0}^{x_1} \eta\frac{d^2}{dx^2}\frac{\partial f}{\partial Y''}\; dx - \cdots (-1)^m \int_{x_0}^{x_1} \eta\frac{d^{(m)}}{dx^{(m)}}\frac{\partial f}{\partial Y^{(m)}}\; dx.$$

Factoring the auxiliary function η out and combining the terms simplifies to

$$\frac{dJ}{d\epsilon} = \int_{x_0}^{x_1} \eta\Big(\frac{\partial f}{\partial Y} - \frac{d}{dx}\frac{\partial f}{\partial Y'} + \frac{d^2}{dx^2}\frac{\partial f}{\partial Y''} - \cdots (-1)^m \frac{d^{(m)}}{dx^{(m)}}\frac{\partial f}{\partial Y^{(m)}}\Big).$$

At the extremum at $\epsilon = 0$ and using the Fundamental Lemma of the Calculus of Variations, we arrive at the *Euler-Poisson Equation*

$$\frac{\partial F}{\partial y} - \frac{d}{dx}\frac{\partial f}{\partial y'} + \frac{d^2}{dx^2}\frac{\partial f}{\partial y''} - \cdots (-1)^m \frac{d^{(m)}}{dx^{(m)}}\frac{\partial f}{\partial y^{(m)}} = 0.$$

1.4 Application: A Proposed Energy Functional

A question that we will face over and over again is the idea of *fairness*. In other words, we want to explore if there is a quantified way to determine whether a curve is "nice". We can use this quantity to compare: Given two curves, which one looks aesthetically better? Functionals have been proposed for decades as a universal measure, or metric, of fairness. In this thesis, we will explore various functionals which are used to describe the "energy" of a curve. The notion of energy is derived from the study of elastic curves, where the functional $\int k(s)^2\ ds$ represents the bending energy of the elastica. The curve is of fixed length and has fixed endpoints, where s denotes the arc-length of the curve and k denotes the (signed) curvature. The functional is often referred to in spline theory as the Minimum Energy Curve, or MEC, and will be explored in further detail later on. However, the MEC does have a few shortcomings which causes it to fail a few desirable properties for splines (such as roundness). Thus, a new functional called the Minimum Variation Curve, or MVC, was proposed. The MVC is represented as the integral of the squared change of curvature, i.e. $\int \dot{k}(s)^2\ ds$. The MVC does satisfy some properties that the MEC fails to (such as roundness). But we wonder if there is another functional that we can propose as a better fairing metric, a better "energy" curve?

We notice that the functional $\int k(s)^2\ ds$ actually belongs to a hierarchy of functionals. The *filament equation* (also called the *Betchov-Da Rios equation* or the *localized induction equation*) is an evolution equation on arc-length parameterized curves $\Gamma(s)$ in $\mathbb{R}^3$ defined as

$$\Gamma' = \dot{\Gamma} \times \ddot{\Gamma},$$

where Γ' is a derivative with respect to time and $\dot{\Gamma}, \ddot{\Gamma}$ are derivatives with respect to arc-length s along the curve Γ. It is a solition equation for space curves, best known as a model for the behavior of thin vortex tubes in an incompressible, inviscid, three dimensional fluid. This is an infinitely dimensional, completely integrable Hamiltonian system [9], [52]. The filament equation possesses infinitely many conserved quantities, all involving integrals in terms of the curvature k and the torsion τ of a curve. This forms a hierarchy of Poisson commuting integrals which start with

$$\int 1\ ds, \quad \int \tau\ ds, \quad \int k^2\ ds, \quad \int k^2\tau\ ds, \quad \int \left(\dot{k}^2 + k^2\tau^2 - \frac{1}{4}k^4\right)\ ds, \ldots$$

Suppose if we take a look at the hierarchy of integrals and examine their stationary functions via calculus of variations. From $\int 1\ ds$, the equilibria are geodesics. The equilibria for the linear combinations of $\int 1\ ds$ and $\int \tau\ ds$ form helices. The equilibria for the linear combinations of $\int 1\ ds$, $\int \tau\ ds$ and $\int k^2\ ds$ form Kirchhoff elastic rods [52]. For the purpose of this paper, we will deal with plane curves in $\mathbb{R}^2$, where the torsion element $\tau = 0$. With this in mind, what about the next one in line that does not completely vanish when $\tau = 0$, $\int \left(\dot{k}^2 - \frac{1}{4}k^4\right)\ ds$? What do equilibria look like and if we minimize this integral, what functions do we expect as a result?

For simplification, multiply that particular integral by $\frac{1}{2}$. Given the functional

$$\mathcal{F} = \int \frac{1}{2}\dot{k}^2 - \frac{1}{8}k^4 \, ds$$

in the plane $\mathbb{R}^2$, we wish to minimize it. For this, we will need to derive the variation formulas for k^2, k^4 and $\dot{k}^2$ by using differential geometry. These derivations will be described and formulated later in the thesis. But after all the work is done, we will have the Euler-Lagrange equation

$$E = \ddot{\ddot{k}} + \frac{5}{2}k^2\ddot{k} + \frac{5}{2}k\dot{k}^2 + \frac{3}{8}k^5 = 0.$$

As for solutions to the Euler-Lagrange equation above, let's assume that a solution has the form

$$\frac{1}{2}\dot{k}^2 = -\frac{1}{8}k^4 + \phi(k).$$

Then ϕ satisfies the third order equation

$$0 = 2\phi'''\phi - \frac{1}{4}k^4\phi''' + \phi''\phi' + k^2\phi' - \frac{1}{2}k^3\phi'' - k\phi, \text{ where } {}' = \frac{d}{dk}$$

which has first integral

$$C = 2\phi\phi'' - \frac{1}{2}\phi'^2 - \frac{1}{4}k^4\phi'' + \frac{1}{2}k^3\phi' - \frac{1}{2}k^2\phi.$$

This has polynomial solutions

$$\phi_1(k; a) = ak^2 + 4a^2 \text{ when } C = 16a^4$$

and

$$\phi_2(k;a) = bk \text{ when } C = -\frac{1}{2}b^2$$

.

Solving $\frac{1}{2}\dot{k}^2 = -\frac{1}{8}k^4 + \phi(k)$ in the case $\phi = \phi_1$ yields the Jacobi elliptic function

$$k = A\text{cn}(\alpha s, p) \text{ where } A = 2\alpha p$$

where the elliptic modulus is

$$p^2 = \frac{3-\sqrt{3}}{6} \text{ or } p^2 = \frac{3+\sqrt{3}}{6}.$$

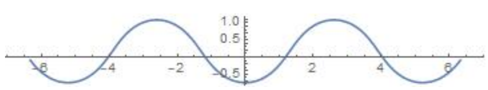

Figure 1.1: $p^2 = \frac{3-\sqrt{3}}{6}$

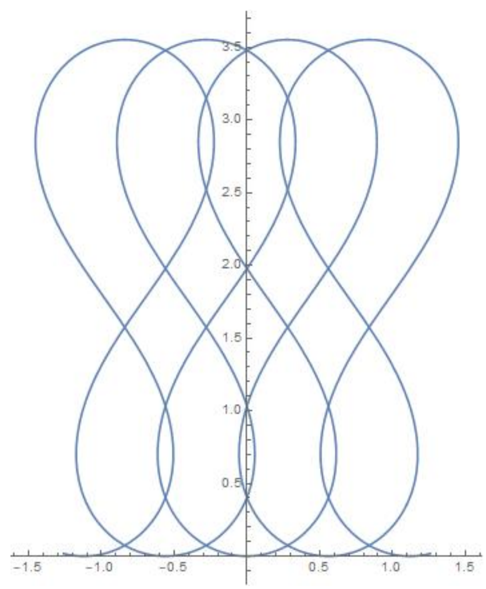

Figure 1.2: $p^2 = \frac{3+\sqrt{3}}{6}$

The corresponding solution curves are certain elastic curves, which we will provide their corresponding graphs [See Figures 1.1 and 1.2]. Solving $\frac{1}{2}\dot{k}^2 = -\frac{1}{8}k^4 + \phi(k)$ in the case of $\phi = \phi_2$ yields the Weierstrass elliptic function

$$k = \frac{1}{\wp(s; 0, \frac{1}{4})}.$$

The corresponding solution curve is the Kiepert trefoil [See Figure 1.3].

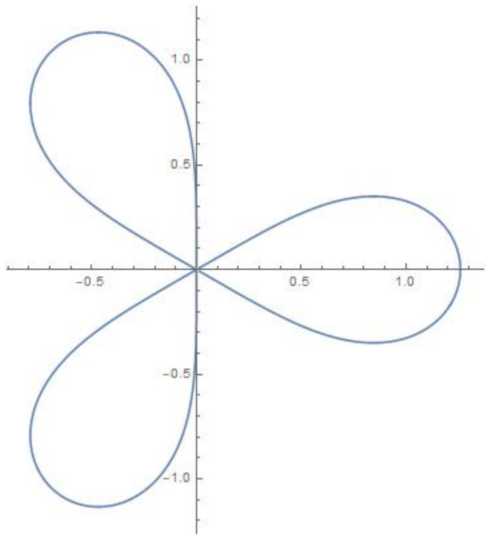

Figure 1.3: The Kiepert Trefoil

The highlight of this thesis will be an analysis of the Kiepert trefoil. The trefoil is a particularly fascinating curve, with many astounding properties. But as we will see, the trefoil is actually a good candidate for a model for a two parameter family of splines. We will derive the reasons why and provide a few examples as to how well pieces of the trefoil can be used to approximate an inscribed circle around a polygon.

Chapter 2

Elliptic Functions

2.1 An Introduction to Elliptic Functions

While elliptic functions and curves do not resemble ellipses, the origin of their name comes from the integral used when calculating the arc length of an ellipse, which was first studied by John Wallis in 1655. Both Wallis and Sir Issac Newton published an infinite series expansion for the arc length of an ellipse. In the late 1700s, Adrien-Marie Legendre began to use elliptic functions in mathematical applications to physics. These applications included the movement of the pendulum and the deflection of a thin elastic bar (which we will explore in the chapter discussing the *elastica*). Legendre spent over forty years of his life working on elliptic functions and the classification of elliptic integrals. His first published writings on elliptic integrals consisted of two papers in 1786. His major work on elliptic functions appeared in a three volume series between 1811 and 1816. He then repeated much of his work in another three volume series, which was published between 1825 and 1830. Despite all of the time, work and dedication he put into this research on elliptic functions, Legendre's work would go unnoticed. Gauss would later make connections between elliptic functions and trigonometric functions, which would also go unnoticed.

That is, until 1827, when Niels Henrik Abel and Carl Gustav Jacob Jacobi revived the subject. Not only they brought life back to the works of Legendre and Gauss, they also utilized elliptic functions into their individual works, advancing the fields of mathematics and physics. Abel discovered how elliptic functions were *doubly periodic* while Jacobi found that elliptic functions were beneficial when it came to integrating second order kinetic energy equations. Jacobi's work showed that the motion equations (in rotational form) are integrable only for the three cases of the pendulum, the symmetric top in a gravitational field and a freely spinning body. All of which have solutions in terms of elliptic functions. In 1862, Karl Weierstrass would generalize the theory of elliptic functions based on his $\wp$-function to show that they can be applied to problems in both algebra and geometry [3]. One of his results was that any elliptic function can be expressed in terms of $\wp$ and its derivative $\wp'$ [22]. In 1890, Alfred Cardew Dixon introduced his elliptic functions which displayed fascinating symmetries with hexagons.

Although not taught in the standard collegiate mathematics curriculum, elliptic functions are still used in many applications today. In physics, they are used to calculate the particle charge from its curved path through a magnetic field. In mechanics, they are used to make calculations about the motion of certain objects. The classic example in mechanics is the motion of pendulums. In astronomy, they are used to define the trajectories of spacecraft. One example was the Dawn probe, which explored the asteroid belt, primarily Ceres and Vesta [3].

Before we define what an elliptic function is, let us recall a few notions from complex analysis. Let D be a connected open set in $\mathbb{C}$. We say that a function $f(z)$ defined on

D is *analytic* if $f'(z)$ exists everywhere in D. In relation to that, we say a function $f : D \to \mathbb{C} \cup \{\infty\}$ is *meromorphic* if whenever $f(a) = \infty$, then a is an isolated point, and there exists a positive integer n such that $\lim_{z\to a}(z-a)^n f(z)$ exists and is nonzero. Such a value a is called a *pole* and n is called the *order* of the pole [83].

Suppose that $f(z)$ is a complex function of one variable. A value L is called a *period* of a function if

$$f(z+L) = f(z)$$

for every z where it is defined. Elementary examples of period functions would be trigonometric functions (for example, $\sin(z)$ and $\cos(z)$ each have a period of 2π). Now suppose that $f(z)$ has two non-parallel periods, ω_1 and $\omega_2 \in \mathbb{C}$, which obeys the following property

$$f(z+\omega_1) = f(z), \quad f(z+\omega_2) = f(z),$$

whose ratio $\frac{\omega_1}{\omega_2}$ is not purely real. Then, the function $f(z)$ is called a *doubly-periodic* function with periods ω_1 and ω_2 (we need this condition to ensure these values correspond to different directions in the complex plane) [68].

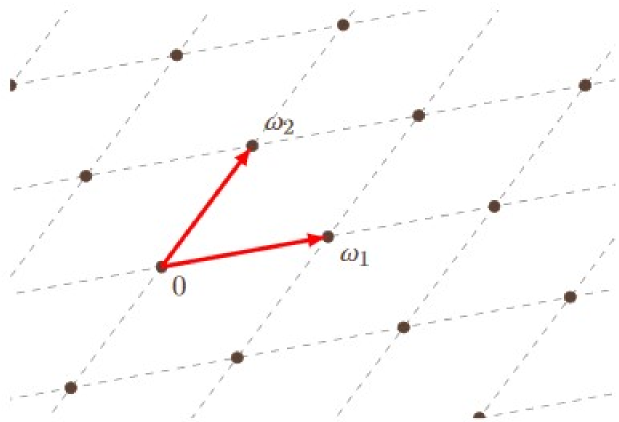

Figure 2.1: The lattice generated by ω_1 and ω_2. Reprinted from [17].

We define a *lattice* to be a module over the integers

$$\Lambda = \mathbb{Z}\omega_1 + \mathbb{Z}\omega_2 := \{m\omega_1 + n\omega_2 : m, n \in \mathbb{Z}\},$$

where $\frac{\omega_1}{\omega_2} \notin \mathbb{R}$. By defining such a lattice, we can see that Λ acts on $\mathbb{C}$ by $(\omega, z) \mapsto z + \omega$ and that all discrete translational subgroups of $\mathbb{C}$ with two independent directions "tile" the complex plane with parallelograms. For instance, the complex numbers $0, \omega_1, \omega_2, \omega_1 + \omega_2$ define a parallelogram on the complex plane. If we choose ω_1, ω_2 to be values of smallest modulus, then we may define a *fundamental parallelogram* for the lattice as a connected, compact subset of $\mathbb{C}$ such that its translates under the action of Λ tiles the plane [See Figure 2.2]. In other words, we define the *fundamental parallelogram* of Λ to be the region F such that

$$F := \{a\omega_1 + b\omega_2 : 0 \leq a, b < 1\}.$$

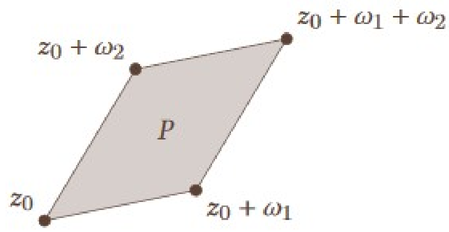

Figure 2.2: A fundamental parallelogram. Reprinted from [17].

We can now formally define an elliptic function. A function $f(z)$ is called *elliptic* if it is meromorphic and is doubly-periodic with respect to Λ. For this thesis, we will focus on three types of elliptic function: Weierstrass, Jacobi and Dixon. Two of the solutions for our proposed functional involve Jacobi elliptic functions and the trefoil can be represented in terms of both Weierstrass and Dixon elliptic functions. We will explore these different types in detail.

2.2 The Weierstrass $\wp$ Function

The first example of an elliptic function is the Weierstrass $\wp$ Function associated with a lattice Λ:

$$\wp = \frac{1}{z^2} + \sum_{\omega \in \Lambda}' \frac{1}{(z - \omega^2)} - \frac{1}{\omega^2}$$

where the prime on the sum (') denotes that the sum excludes terms with a denominator of zero. It can be shown that $\wp$ is indeed an elliptic function. More than that, $\wp$ is an even function with a double pole at each lattice point. Even more astounding is that any elliptic function can be written as a rational function of $\wp(z)$ and its derivative, $\wp'(z) = -2 \sum_{\omega \in \Lambda} \frac{1}{(z-\omega)^3}$.

Define the *modular invariants* of the lattice as

$$g_2 = 60 \sum_{\omega\in\Lambda}{}' \frac{1}{\omega^4} \quad \text{and} \quad g_3 = 140 \sum_{\omega\in\Lambda}{}' \frac{1}{\omega^6}.$$

Then, we can derive the first few terms of the Laurent series of $\phi(z)$ at $z = 0$:

$$\begin{aligned}
\wp(z) &= \frac{1}{z^2} + \sum_{\omega\in\Lambda}{}' \frac{1}{\omega^2}\left(\left(1 - \frac{z}{\omega}\right)^{-2} - 1\right) \\
&= \frac{1}{z^2} + \sum_{\omega\in\Lambda}{}' \sum_{n=1}^{\infty} \frac{1}{\omega^{n-2}}(n+1)z^n \\
&= \frac{1}{z^2} + \sum_{n=1}^{\infty} z^n(n+1) \sum_{\omega\in\Lambda}{}' \frac{1}{\omega^{n+2}} \\
&= \frac{1}{z^2} + \frac{g_2}{20}z^2 + \frac{g_3}{28}z^4 + O(z^6)
\end{aligned}$$

Note that the order of the summation can be interchanged since the series converges uniformly on a compact neighborhood of the origin. The odd terms cancel out due to $-\omega$ and ω are both in the lattice, so raising both to an odd power causes them to cancel in the sum [17]. Using this expansion of $\wp$ and some rather tedious calculation, the following theorem is proven in Chapling [17]:

Theorem 2.2.1 *$\wp$ and its derivative $\wp'$ satisfy the following nonlinear differential equation:*

$$\wp'^2 = 4\wp^3 - g_2\wp - g_3.$$

and its corollary

Corollary 2.2.2 *$\wp$ is the inverse of the elliptic integral*

$$\int_0^z \frac{dw}{\sqrt{w^3 - g_2 w - g_3}}.$$

2.3 The Jacobi Elliptic Function

The most common type of elliptic functions are the *Jacobi elliptic functions*. These functions parallel trigonometric functions, except that the unit circle is replaced with an ellipse. William A. Schwalm gives a detailed, algebraic argument for the derivation of the Jacobi elliptic functions in his lecture series [72]. For this paper, we will base the derivation on the inversion of a particular elliptic integral.

The three standard Jacobi elliptic functions are the *elliptic sine* $\mathrm{sn}(u,k)$, the *elliptic cosine* $\mathrm{cn}(u,k)$ and the *delta amplitude* $\mathrm{dn}(u,k)$. These functions are derived from the inversion of the elliptic integral of the first kind

$$F = \int_0^z \frac{dz}{\sqrt{1-z^2}\sqrt{1-k^2z^2}}.$$

We let

$$u = F(\phi, k) = \int_0^\phi \frac{dt}{\sqrt{1-k^2\sin^2 t}}$$

where $0 \le k^2 \le 1$ and the upper bound on the elliptic integral F is often referred to as the *Jacobi amplitude*, or am for short. The inversion of the elliptic integral yields

$$\phi = F^{-1}(u,k) = \mathrm{am}(u,k).$$

From this, we can officially define the Jacobi elliptic functions:

$$\sin\phi = \sin(\mathrm{am}(u,k)) = \mathrm{sn}(u,k)$$

$$\cos\phi = \cos(\mathrm{am}(u,k)) = \mathrm{cn}(u,k)$$

$$\sqrt{1-k^2\sin^2\theta} = \sqrt{1-k^2\sin^2(\mathrm{am}(u,k))} = \mathrm{dn}(u,k)$$

Note that if the context makes clear as to what k is, then we may omit the modulus $(\mathrm{sn}(u), \mathrm{cn}(u), \mathrm{dn}(u))$ when writing these functions to make calculations less messy.

Some immediate consequences of the Jacobi elliptic definitions defined above are

$$\mathrm{sn}^2(u) + \mathrm{cn}^2(u) = 1, \quad k^2\mathrm{sn}^2(u) + \mathrm{dn}^2(u) = 1, \quad \mathrm{sn}(0) = 0, \quad \mathrm{cn}(0) = \mathrm{dn}(0) = 1.$$

In total, there are twelve Jacobian elliptic functions, where the remaining nine can be defined by the ratios of the three we have already defined. Before we start, one may be tempted to relate standard trigonometry and state that $\frac{\mathrm{sn}(u)}{\mathrm{cn}(u)} = \mathrm{tn}(u)$ for some tangent equivalence to elliptic functions. While in some texts that is done, there is a nicer notation devised by Gudermann and Glaisher in which the reciprocals are indicated by reversing the letters [72]:

$$\mathrm{ns}(u) = \frac{1}{\mathrm{sn}(u)}, \quad \mathrm{nc}(u) = \frac{1}{\mathrm{cn}(u)}, \quad \mathrm{nd}(u) = \frac{1}{\mathrm{dn}(u)}.$$

Also, the ratios are named by catenation of the first letters, and so

$$\mathrm{sc}(u) = \frac{\mathrm{sn}(u)}{\mathrm{cn}(u)}, \quad \mathrm{cs}(u) = \frac{\mathrm{cn}(u)}{\mathrm{sn}(u)}, \quad \mathrm{sd}(u) = \frac{\mathrm{sn}(u)}{\mathrm{dn}(u)}$$

$$\mathrm{ds}(u) = \frac{\mathrm{dn}(u)}{\mathrm{sn}(u)}, \quad \mathrm{cd}(u) = \frac{\mathrm{cn}(u)}{\mathrm{dn}(u)}, \quad \mathrm{dc}(u) = \frac{\mathrm{dn}(u)}{\mathrm{cn}(u)}.$$

2.4 The Dixon Elliptic Functions

In 1890, Alfred Cardew Dixon introduced a series of elliptic functions on the complex plane which parameterized the Hessian cubic curve

$$x^3 + y^3 - 3axy = 1.$$

For the purpose of this paper, we would like to focus on the case of the Fermat cubic curve where $a = 0$, which produces the Fermat cubic curve. The entire complex plane can be tiled by regular hexagons such that the restriction of the function to such a hexagon is a shift of its restriction to any of the other hexagons. Going back with how elliptic functions were defined, the Dixon elliptic functions do not contradict the notion that a doubly periodic meromorphic function has a fundamental parallelogram. This is due to the vertices of such a parallelogram may be taken to be the centers of four suitable selected hexagons [82].

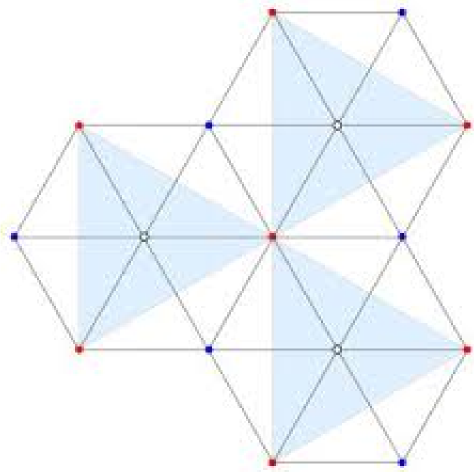

Figure 2.3: The entire complex plane can be tiled by regular hexagons. Reprinted from [55].

The *Dixonian sine function* $w = \mathrm{sm}(z)$ is implicitly defined as the inverse of the equation

$$z = \int_0^w \frac{dx}{(1-x^3)^{\frac{2}{3}}}.$$

The *Dixonian cosine function* $\mathrm{cm}(z)$ is defined by the relation

$$\mathrm{sm}^3(z) + \mathrm{cm}^3(z) = 1.$$

From these definitions, one can easily show that

$$\mathrm{sm}(0) = 0, \qquad \mathrm{cm}(0) = 1$$

along with their derivatives

$$\frac{d}{dz}\mathrm{sm}(z) = \mathrm{cm}^2(z), \qquad \frac{d}{dz}\mathrm{cm}(z) = -\mathrm{sm}^2(z).$$

The Dixonian elliptic functions can also be defined in terms of the Weierstrass elliptic function $\wp$ and its derivative $\wp'$:

$$\mathrm{sm}(z) = \frac{6\wp(z;0,\frac{1}{27})}{1 - 3\wp'(z;0,\frac{1}{27})}$$

and

$$\mathrm{cm}(z) = \frac{3\wp'(z;0,\frac{1}{27}) + 1}{3\wp'(z;0,\frac{1}{27}) - 1}.$$

The Dixonian elliptic functions have periods of $3K$ and $3\omega K$ where

$$\omega = \frac{-1 + i\sqrt{3}}{2}$$

is a cube root of unity and for $j = 0, 1, 2, ...$

$$\mathrm{sm}(z + 3\omega^j K) = \mathrm{sm}(z), \qquad \mathrm{cm}(z + 3\omega^j K) = \mathrm{cm}(z).$$

Chapter 3

Splines, Their Properties and a Criterion for Suitable Splines

3.1 Splines and Their Properties

What is a spline curve? A *spline curve* in the plane is a curve passing consecutively through a specified set of points $P_1, P_2, ..., P_n$, called knots. The segment of the curve joining P_i and P_{i+1} is a smooth curve, but the entire curve is typically piecewise smooth, with at least a tangent line at each knot (See Figure 3.1). While most mathematical descriptions of splines assume each piece is given by polynomials, we will be interested in more general ("nonlinear") splines. In fact, the original spline used by draftsmen was a flexible strip of wood, and the resulting curve was an elastica. We will be considering splines defined by a variational criterion.

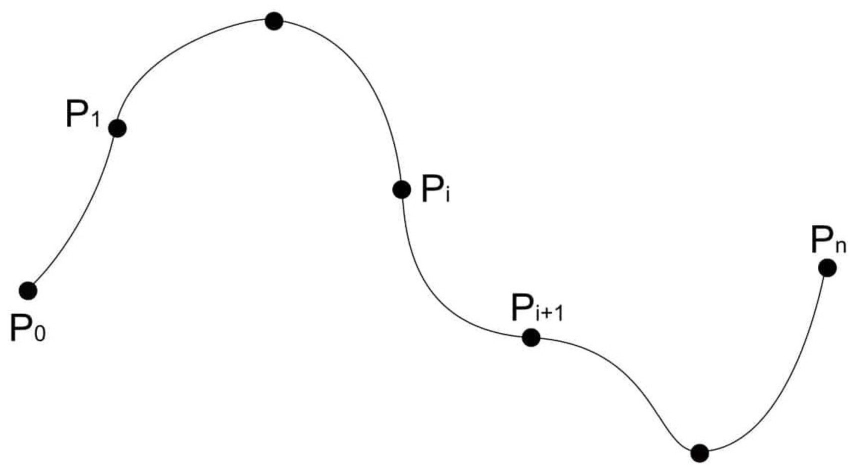

Figure 3.1: An example of a spline.

Given a set of points, the set of all possible interpolating splines that go through these points are infinite. We would like to narrow down the list to only include the ones which are the "best". But as of this time, there is no agreement as to what qualifies as the "best" spline. Raph Levien lists a number of ideal properties that would be desirable for splines to have. But be forewarned. Some splines do not exist for an arbitrary sequence of points and a number of desirable properties may not apply to all splines [57].

In most of the literature pertaining to splines, the one property that comes up repeatedly is *fairness*, which is essentially the notion of smoothness. Fairness is more of an aesthetic property, opposed to a mathematical one since fairness depends on how humans perceive curves. But there are some metrics which correlate reasonably well to the notion of fairness. One such metric is *curvature*, which also has a mathematical association with how much a curve deviates from a straight line. But the human mind is fickle since we perceive curves with regions of extremely high curvature not fair, as with curves with discontinuities in curvature or regions of curvature variation.

Another property related to fairness is the idea of *continuity*, i.e. how many higher derivatives of a curve exists. Continuity can be divided into two classes: *parametric* and *geometric*. *Parametric continuity* refers to the smoothness of both the curve itself and its parametrization, denoted as C^k. A curve is C^k continuous if all partial derivatives up to order k exist and are continuous. *Geometric continuity* refers to the smoothness of a curve that is independent of any curve parametrization, denoted as G^k. For instance:

G^0 (Positional continuity): The curve meets at each joint point.

G^1 (Tangent continuity): The curve share a common tangent direction at each joint point.

G^2 (Curvature continuity): The curve share a common center of curvature at each joint point.

G^3 (Torsion continuity): The curve share a common rate of change of curvature at each joint point.

As we can see, parametric continuity is stronger than geometric since parametric requires the derivatives at each joint point to be continuous where geometric only requires the tangents at each joint to be continuous. Keep in mind that just because a curve is continuous does not necessarily mean that it is fair. A typical counter example would be the Euler spline (which has G^2 continuity) compared to the circle spline (which has G^3 continuity). The Euler spline is more fair than the circle spline since it has less variation in the curvature.

A specific aspect to fairness is the notion of *roundness*, i.e. the idea that a spline will yield a circular arc when the points are co-circular. Intuitively, the circle should be the fairest curve due to their common occurrence in nature. However, remember that many splines are approximations with some doing a much better job than others. Also note that if one uses a spline based on polynomials, it will never be exactly round. It should be noted that some splines are too sensitive for the roundness condition to apply. A common technique used to handle these cases is to normalize the parametrization by the chord length. However, this is done at a price since the extensionality of the spline is compromised.

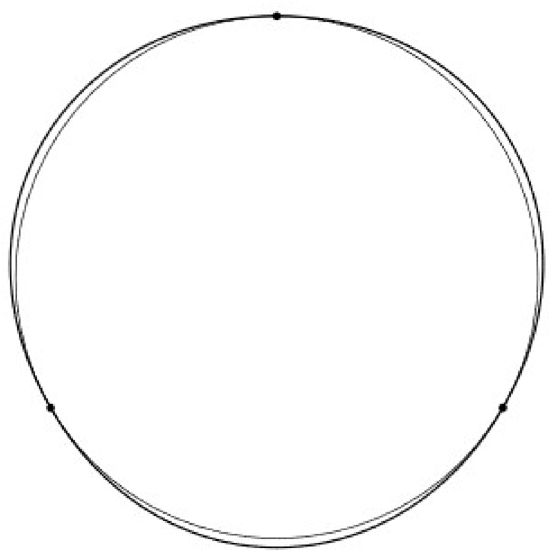

Figure 3.2: Roundness failure. Reprinted from [57].

Extensionality is a property that explores the local (and in turn, the global) behavior of the spline. While often used as a filter to weed out crude approximations, extensionality is useful to determine whether or not a certain spline curve is optimal. Suppose an additional data point is added to the spline. Will the shape of the curve change or will it remain the same? This notion is closely related to choosing an optimal curve based on some fairness metric. This is because if the shape of the spline changes with the introduction to a new data point, then either the original curve or the new one must have not been optimal.

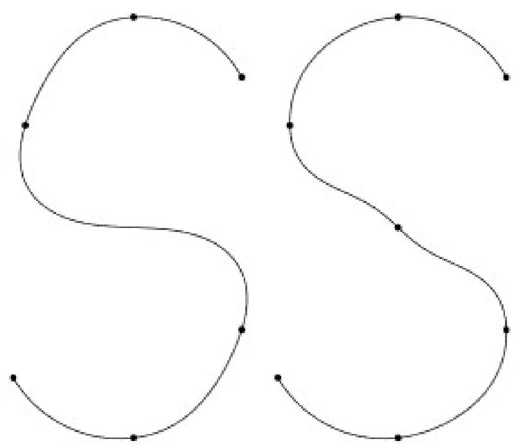

Figure 3.3: The circle spline fails at extensionality. Reprinted from [57].

Where extensionality focuses on the addition of a data point, *locality* explores what happens if a particular data point moves. How much of the resulting curve will change? Will it be a small local region where the shift took place or will it be the entire spline? Some splines have a property called *finite support*, where moving a data point changes the curve only for a section bracketed by a finite number of points on either side of the one moved. However, this conflicts with extensionality directly. For this reason, locality is measured by how quickly the effect of moving a point dies out as one moves further away from it. One can assume the higher the degree of geometric continuity a curve possesses, the more fair the curve would look. But this assumption actually *decreases* locality and can cause discontinuities to be more visible. According to literature based on the fairness of splines, it is required that the spline should be at least G^2 continuous.

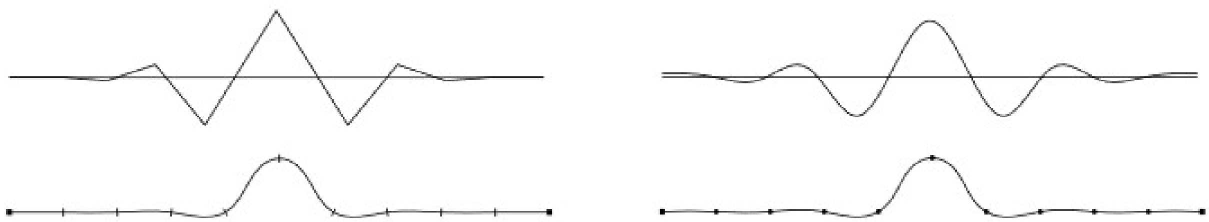

Figure 3.4: G^2 spline (on the left) has better locality than G^4 spline (on the right). Reprinted from [57].

One desirable property of splines is for them to be invariant to transformations. All functions worthy of being considered as splines should have some form of *transformational invariance*, i.e. unchanged under rigid transformations such as rotation, (uniform) scaling and translation. A sometimes equally desirable property is *affine invariance* or *affinity*, which preserves the shape of the spline. Recall that affinities are transformations which preserve points, straight lines and planes. These transformations include homothety, reflection, rotation, scaling, shear mapping, similarity transformation and translation. Affinity is observed in many polynomial based splines but it often conflicts with roundness. So more often than not, roundness is considered by many authors as the better trade-off.

3.2 Parameters of Splines and a Criterion for Suitable Splines

One can count how many parameters does the spline depend on, since the family of curve segments between any two points is potentially drawn from an infinite space. But in practice, most splines use segments chosen from a finite dimensional manifold (which will be defined in Chapter 5). In general, there is a vector of real parameters that uniquely determines the shape of the curve between any two endpoints. By counting these parameters, we can hold the endpoints of each segment fixed and apply the rotation, scaling and translation to make the curve coincide with the endpoints. The common types of parameters in recent papers about spline interpolation are the *two-parameter* and the *four-parameter* variety.

A *two-parameter* spline is a spline such that every interpolating curve segment between two adjacent knots is uniquely determined by the two angles between tangent and chord at the endpoints of the segment. In his thesis, Levien showed that there was a special relationship between two-parameter and extensional splines. He found that all two-parameter extensional splines correspond to a single generating curve, where segments between adjacent knots can be cut from such a curve (subject to scaling, rotation, translation and mirror image transformations). This is done so that the endpoints of the cut segments can be aligned with the endpoints in the spline. In addition to that, any generating curve can be used as the basis of a two-parameter extensional spline [57]. This is stated in his theorem:

Theorem 3.2.1 (R.L. Levien, 2009)

In an extensional, G^2-continuous, two-parameter spline, there exists a curve such that for any spline segment (parametrized by angles θ_0 and θ_1) there exist two points on the curve (s_0 and s_1) such that the segment of the curve, when transformed by rotation, scaling and translation so that the endpoints coincide, also coincides along the length of the segment.

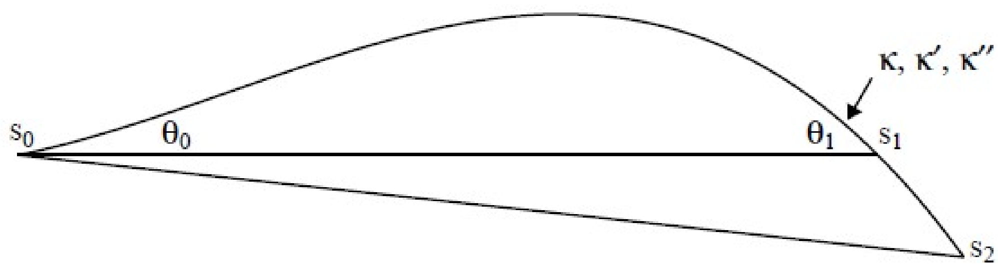

Figure 3.5: Construction of the generator curve of a two-parameter spline. Reprinted from [57].

Levien states that the proof to this theorem revolves around the quantity $\dot{k}/k^2$, which he asserts is limit of the quantity $6(\theta_1 - \theta_0)/(\theta_0 + \theta_1)^2$ as both θ_0 and θ_1 approach zero (i.e. as the length of the curve segment becomes infinitesimal). This particular quantity represents how much curvature variation there is for a segment for a fixed curvature. However, there are some limitations to the derivation. In addition to that, we wonder if there is a special geometric meaning behind the quantity $\dot{k}/k^2$. With this in mind, we present a more mathematically rigorous explanation which gives a direct meaning behind that quantity for any arbitrary curve.

First, let $X(t)$ be a smooth curve defined on an interval $[a, b]$. Assume that the curvature k satisfies the condition $\dot{k}/k^2$ is a strictly monotonic function on (a, b), where $\dot{k}$ is the derivative of k with respect to arc length.

Theorem 3.2.2 (T.A. Clark)

Given $a < u < v < b$ and let V be the secant line from $X(u)$ to $X(v)$.

Let $\theta_0 > 0$ be the angle between the tangent vector $T(v)$ at $X(v)$ and V.

Likewise, let $\theta_1 > 0$ be the angle between the tangent vector $T(u)$ at $X(u)$ and V.

Then for any sufficiently close pair of angles θ_0' and θ_1', there exists a unique nearby pair of points $X(u')$ and $X(v')$ such that the corresponding secant line achieves these angles.

Proof .

We define the secant line that passes through $X(v)$ and $X(u)$ as a unit vector by the following:

$$V = \frac{X(u) - X(v)}{\|X(u) - X(v)\|} = \frac{X(u) - X(v)}{r} = \frac{X_{10}}{r}$$

where

$$X_{10} = X(u) - X(v)$$

and

$$r = \|X_{10}\| = \|X(u) - X(v)\|.$$

We will define the angles formed by V and the tangent vectors at each endpoint by:

$$\sin\theta_0 = \langle V, N(v)\rangle \quad \text{and} \quad \sin\theta_1 = \langle V, N(u)\rangle$$

where

$$N(s) = N(0) - sk(0)T(0) + \frac{s^2}{2}(-\dot{k}T(0) - k^2N(0)) + \cdots .$$

We define the following function:

$$F(v, u) = (\theta_0, \theta_1) = (\arcsin\langle V, N(v)\rangle, \arcsin\langle V, N(u)\rangle).$$

We now find the Jacobian J of this multivariable function where

$$J = \begin{vmatrix} \frac{\partial}{\partial u}\theta_0 & \frac{\partial}{\partial v}\theta_0 \\ \frac{\partial}{\partial u}\theta_1 & \frac{\partial}{\partial v}\theta_1 \end{vmatrix}.$$

where

$$
\begin{aligned}
\frac{\partial}{\partial u}\theta_0 &= \frac{1}{\cos\theta_0}\Big(-\frac{1}{r^3}\langle T(u), X_{10}\rangle\langle X_{10}, N(v)\rangle + \frac{1}{r}\langle T(u), N(v)\rangle\Big) \\
\frac{\partial}{\partial v}\theta_0 &= \frac{1}{\cos\theta_0}\Big(\frac{1}{r^3}\langle T(v), X_{10}\rangle\langle X_{10}, N(v)\rangle + \frac{1}{r}\langle X_{10}, -k(v)T(v)\rangle\Big) \\
\frac{\partial}{\partial u}\theta_1 &= \frac{1}{\cos\theta_1}\Big(-\frac{1}{r^3}\langle T(u), X_{10}\rangle\langle X_{10}, N(u)\rangle + \frac{1}{r}\langle X_{10}, -k(u)T(u)\rangle\Big) \\
\frac{\partial}{\partial v}\theta_1 &= \frac{1}{\cos\theta_1}\Big(\frac{1}{r^3}\langle T(v), X_{10}\rangle\langle X_{10}, N(u)\rangle + \frac{1}{r}\langle -T(v), N(u)\rangle\Big)
\end{aligned}
$$

where

$$
\frac{\partial}{\partial u}\Big(\frac{1}{r}\Big) = -\frac{1}{r^3}\langle T(u), X(u) - X(v)\rangle \quad \text{and} \quad \frac{\partial}{\partial v}\Big(\frac{1}{r}\Big) = \frac{1}{r^3}\langle T(v), X(u) - X(v)\rangle.
$$

For the Jacobian, we wish to find in which case(s) does $J \neq 0$. We wish to show that the derivative of the function F is non-singular and is locally homeomorphic near 0. To make the Jacobian a bit easier to calculate, we will change the variables from (v, u) to $(v, v+e)$. This means we are in the half plane $e > 0$. We will also fix v at 0 and let e become s. So by the change of variables, we transform (v, u) to $(0, s)$. By using Taylor series centered at 0 and truncating all expansions to the cubic term, we arrive at the following computations:

$$
\begin{aligned}
X(s) - X(0) = rV = sT + \frac{s^2}{2}kN + \frac{s^3}{6}(\dot{k}N - k^2T) \\
T(s) = T + skN + \frac{s^2}{2}(\dot{k}N - k^2T) + \frac{s^3}{6}((\ddot{k} - k^3)N - 3k\dot{k}T) \\
N(s) = N - skT + \frac{s^2}{2}(-\dot{k}T - k^2N) - \frac{s^3}{6}((\ddot{k} - k^3)T + 3k\dot{k}N)
\end{aligned}
$$

where

$$T = T(0), \quad N = N(0), \quad k = k(0), \quad \dot{k} = \dot{k}(0) \quad \text{and} \quad \ddot{k} = \ddot{k}(0).$$

Then, by making the necessary substitutions and dot products, we have

$$J = \frac{\frac{1}{12}(2\dot{k}^2 - k\ddot{k})s^8 + \frac{1}{24}\dot{k}(k^3 + 2\ddot{k})s^9 + \frac{1}{24}k^3\ddot{k}s^{10}}{r^6 \cos\theta_0 \cos\theta_1}.$$

Since the angles are small when s is small, we can use the small angle approximations for cosine which yield the product $\cos\theta_0 \cos\theta_1 \approx 1$. The value r^2 is approximately s^2 when s is small, and so r^6 is approximately s^6 when s is small. Thus, we can estimate J by a polynomial of lowest order term s^2

$$J \approx \frac{1}{12}(2\dot{k}^2 - k\ddot{k})s^2 + \frac{1}{24}\dot{k}(k^3 + 2\ddot{k})s^3 + \frac{1}{24}k^3\ddot{k}s^4.$$

If $s = 0$, the Jacobian is singular. But if $s \neq 0$ but is sufficiently small, the higher order terms are irrelevant and the lowest order term $\frac{1}{12}(2\dot{k}^2 - k\ddot{k})s^2$ dominates.

The assumption that $\dot{k}/k^2$ is strictly monotonic means that

$$\frac{d}{ds}\left(\frac{\dot{k}}{k^2}\right) = \frac{k^2\ddot{k} - 2k\dot{k}^2}{k^4} = -\frac{2\dot{k}^2 - k\ddot{k}}{k^3} \neq 0.$$

Thus, $J \neq 0$.

∎

Keep in mind that because we used a Taylor expansion for the curve and for the tangent and normal vectors, this does not give us a global result. Rather this is a local result but for the sake of splines, we are more concerned with local properties so this is fine.

There are a number of desirable splines which are extensional but do not fit into a two-parameter space, rather they require the use of four parameters. A *four-parameter* spline is a spline in which is determined by both tangent angles and curvatures at the endpoints. Four parameters are needed when one wishes for a spline or to study a surface with greater than G^2-continuity. They are useful due to many shapes are not best represented as a simple interpolating spline, such as various fonts designs. With annotating curves with additional constraints, the improvement of the locality property is possible. As noted by Levien, constraints that propagate curvature derivatives in one direction, but leave the parameters unconstrained on one side can isolate sections of extreme changes of curvature, so that those sections do not influence nearby regions of gentle curvature change [57].

Chapter 4

The Minimum Energy Curve and The Minimum Variation Curve

4.1 The Minimum Energy Curve

The Minimum Energy Curve (MEC) is the mathematical idealization of a flexible strip that is constrained to go through all the control points, so that the strip can slide freely. This curve minimizes the bending energy. Mathematically, the MEC is the curve which minimizes the following functional:

$$E_{MEC} = \int_0^l k^2 \, ds.$$

Lee and Forsythe, who both did extensive work with the MEC, showed that the spline can be defined as piecewise segments of the rectangular elastica between each pair of adjacent control points, with G^2 continuity across them. It was proposed that the bending energy would make a good fairness metric. While it is the optimum of the bending energy, this does not make the best spline. The MEC is a two-parameter, extensional spline. So, the shape of the curve above any given chord can be completely determined by the two tangent directions of the curve at either end of the chord. Despite having such desirable properties, it lacks in roundness and robustness. But most of all, it does not accurately predict perceived smoothness. This key result was discovered by Raph Levien in his thesis, where he conducted a survey where he asked participants to pick from a family of curves to determine which one was more fair to them. He found that the concept of fairness is fuzzy at best and varies based on who is being asked [57]. The MEC also fails to be scale invariant, meaning that zooming in and out and redoing the calculation does not produce the same curve [16]. While the MEC does not make an optimal spline, it is still a fascinating curve to study.

4.2 A History on the Elastica

So...what are these *elastic curves*? Well, the study of them trace back to 1691 when Jacob Bernoulli observed the shape of a thin elastic rod under a heavy load until the two ends are perpendicular to a given line. We will also assume that the beam will recover its original shape once the load is removed. Let $\gamma(s) = (x(s), y(s))$ be a parametrization of the centerline of the beam.

In 1694, Jacob Bernoulli stated his solution as the following system of differential equations

$$dy = \frac{x^2}{\sqrt{1-x^4}}\,dx$$
$$ds = \frac{1}{\sqrt{1-x^4}}\,dx$$

with an additional hypothesis where the bending moment is directly proportional to some constant related to the composition of the bar and inversely proportional to the radius of curvature [29]. This idea led to the creation of elliptic functions, which were discussed back in Chapter 3. The problem was then attempted again forty years later by his nephew Daniel Bernoulli and Leonhard Euler. In 1742, Daniel had suggested to Euler a method to figure out the shape of an elastic rod under pressure at both ends. He suggested the way to achieve this was to minimize the following integral

$$\int_0^L \frac{1}{R^2}\, ds$$

where s is the arc length, R is the radius of curvature and L is the length of the elastic rod. The solution to this variational problem (defined in the next section) is called an *elastica*. More formally, an elastica (or elastic curve) is a regular curve γ, with fixed endpoints and fixed tangent vector at the endpoints, which is critical of the functional

$$\mathcal{F}^{\lambda}(\gamma) = \int_0^L (k^2 + \lambda)\, ds,$$

where λ is a length penalty. Note that when $\lambda = 0$, the curve γ is called a *free elastica*.

The main focus of the elastic curve problem is to minimize the energy function defined as the integral of the squared curvature for a curve of a fixed length subjected to boundary conditions. Additional progress on this problem was established over the years. One essential work in elastica was credited to both Joel Langer and David Singer with their study of all closed elastic curves in Euclidean space. They explored the elastica in Euclidean space and classifed the elastic curves in a Riemannian manifold with constant sectional curvature G.

We would like to begin by asking how do we apply variations onto a curve? Exactly, what is a variational problem? A variational problem can be summed up in two descriptions. On one hand, it is something we wish to study how it is changing. On the other hand, it is an "admissible" action, a way to do the change such that the action is isometry invariant (deformations of the object that involve bending without stretching, thus leaving the intrinsic distances undisturbed) [29], [77].

For the purpose of elastic curves, we will consider the following set:

$$C = \{\gamma : [a,b] \to M | \gamma(a_i) = \alpha_i, \gamma'(a_i) = \alpha_i'\}.$$

This represents the the set of functions which have fixed length and boundary conditions (some sources will refer to this as "nailed" curves since they have the same endpoints) [29, 75]. We will then consider the functional

$$\mathcal{F} = \int_\gamma k(s)^2 ds = \int_a^b k(t)^2 v dt,$$

where γ is an immersed curve where $\|\gamma'(t)\| = \frac{ds}{dt} := v \neq 0$, s is the arc length parameter and k is the curvature function. We wish to find the critical points of this functional, which will minimize the bending energy of it.

The derivations that we will need to find the Euler-Lagrange equation of the MEC functional can be drawn from observations of a curve on a Riemannian manifold. But since we are only dealing with planar curves, we will reduce all of the work down to two-dimensions, $\mathbb{R}^2$.

The *covariant derivative* $\nabla_X Y$ measures the derivative of a vector field Y in the direction of a vector X. But since we are dealing with planar curves, the covariant derivative is the same as the ordinary derivative. For vector fields X, Y and Z on $\mathbb{R}^2$, the Lie Bracket $[X, Y]$ is represented by:

$$[X, Y] = \nabla_X Y - \nabla_Y X.$$

We will also need the following formula:

$$\nabla_{[X,Y]} Z = \nabla_X \nabla_Y Z - \nabla_Y \nabla_X Z,$$

where this represents the vanishing curvature of the plane.

Let γ be an immersed curve in $\mathbb{R}^2$. Then, it has velocity vector $V = \gamma' = vT$ and squared geodesic curvature $k^2 = \|\nabla_T T\|^2$. Let τ represent the torsion. From this, we can get the Frenet equations for a curve:

$$\begin{aligned}
\gamma' &= vT \\
\frac{dT}{ds} &= \nabla_T T = kN \\
\frac{dN}{ds} &= \nabla_T N = -kT + \tau B \\
\frac{dB}{ds} &= \nabla_T B = -\tau N
\end{aligned}$$

We will denote by γ a *variation*, defined as:

$$\gamma : (-\epsilon, \epsilon) \times I \to M$$
$$(w, t) \to \gamma(w, t) = \gamma_w(t)$$

with $\gamma(0, t) = \gamma(t)$. For a family of curves $\gamma_w(t) = \gamma(w, t)$, we can write

$$W = W(w, t) = \frac{\partial \gamma}{\partial w}$$
$$V = V(w, t) = \frac{\partial \gamma}{\partial t} = v(w, t)T(w, t)$$

We can say that s represents the arc-length, V is our velocity, $v = \frac{ds}{dt}$ is the speed, and W represents an infinitesimal variation of the curve. Note that $s \in [0, L]$ and in order for the critical curve of the functional to be an elastic curve, the variation field must satisfy the following conditions [67]

$$W(0) = 0, \nabla_T W(0) = 0$$

and

$$W(L) = 0, \nabla_T W(L) = 0.$$

4.3 A Geometric Approach to Minimization

The study of elastic curves within a general Riemannian manifold has been explored by Joel Langer and David Singer [54], [75]. We begin by letting $\gamma : [a, b] \to M$ be an immersed curve where $\|\gamma'(t)\| = \frac{ds}{dt} := v \neq 0$ such that s is the arc length parameter. Let k be the curvature function, where $k \neq 0$ (we assume this for if $k = 0$, then γ

would be a straight line, which isn't very interesting). Let τ represent the torsion and $\{T, N, B\}$ be the orthonormal Frenet frame along γ.

We begin by stating a lemma:

Lemma 4.3.1 *Let M be an n-dimensional Riemannian manifold and $\gamma(w,t)$ be a variation of γ. Then the following formulas hold:*

(i) $[W, V] = 0$

(ii) $W(v) = \langle \nabla_T W, T\rangle v = -gv$*, where* $g = -\langle \nabla_T W, T\rangle$

(iii) $[W, T] = gT$

(iv) $R(W,T)T = \nabla_W \nabla_T T - \nabla_T \nabla_W T - \nabla_{[W,T]} T$*, where R is the Riemann curvature tensor*

(v) $\nabla_W T = \nabla_T W + [W, T]$

(vi) $W(k^2) = 2k\langle \nabla_T^2 W, N\rangle + 2k\langle R(W,T)T, N\rangle + 4gk^2$

Many of these we can show by direct computation. We can see that

$$0 = [W, V] = [W, vT] = W(v)T + v[W, T]$$

by the product rule of Lie Brackets, i.e. $[X, fY] = X(f)Y + f[X, Y]$, given a smooth real-valued function f defined on a manifold M with given vector fields X and Y. And so, we can use algebraic manipulation to show that

$$[W, T] = -\frac{W(v)}{v} T = gT, \text{ where } g = -\frac{W(v)}{v}.$$

Furthermore, we can show that

$$\begin{aligned}
2vW(v) = W(v^2) &= W\langle V, V\rangle \\
&= 2\langle \nabla_W V, V\rangle = 2\langle \nabla_V W, V\rangle \\
&= 2\langle \nabla_{vT} W, vT\rangle = 2v^2\langle \nabla_T W, T\rangle.
\end{aligned}$$

So by the last two derivations, we can see that $g = -\langle \nabla_T W, T\rangle$. But recall from the Frenet frame that $\nabla_T T = kN$ since $\nabla_T T$ is the derivative of the tangent vector T in the direction of the tangent vector. So we can see that $k^2 = \langle kN, kN\rangle = \langle \nabla_T T, \nabla_T T\rangle$ (since $\langle N, N\rangle = 1$). Using that knowledge, we can show that:

$$\begin{aligned}
\frac{\partial k^2}{\partial z} &= W(k^2) = 2\langle \nabla_W \nabla_T T, \nabla_T T\rangle \\
&= 2\langle \nabla_T \nabla_W T + \nabla_{[W,T]} T + R(W,T)T, \nabla_T T\rangle \\
&= 2\langle \nabla_T(\nabla_T W + [W,T]) + \nabla_{[W,T]} T + R(W,T)T, \nabla_T T\rangle \\
&= 2\langle \nabla_T^2 W + \nabla_T(gT) + g\nabla_T T + R(W,T)T, \nabla_T T\rangle \\
&= 2\langle \nabla_T^2 W, \nabla_T T\rangle + 2g\langle \nabla_T T, \nabla_T T\rangle + 2\langle R(W,T)T, \nabla_T T\rangle + 2g\langle \nabla_T T, \nabla_T T\rangle \\
&= 2\langle \nabla_T^2 W, \nabla_T T\rangle + 2\langle R(W,T)T, \nabla_T T\rangle + 4g\langle \nabla_T T, \nabla_T T\rangle \\
&= 2k\langle \nabla_T^2 W, N\rangle + 2k\langle R(W,T)T, N\rangle + 4gk^2 \quad \text{since } \nabla_T T = kN
\end{aligned}$$

We know that

$$\frac{\partial k^2}{\partial z} = 2k\frac{\partial k}{\partial z},$$

which implies (from the work above) that

$$\frac{\partial k}{\partial z} = W(k) = \langle \nabla_T^2 W, N\rangle + \langle R(W,T)T, N\rangle + 2gk.$$

In what follows $\gamma : [0,1] \to M$ will be a curve of length L. For a fixed constant λ, consider the functional

$$\mathcal{F}^{\lambda}(\gamma) = \frac{1}{2}\int_0^L (k^2 + \lambda)\, ds.$$

We want to find the critical values of this functional. Recall, in the beginning of the section, that $v(t) = \frac{ds}{dt}$. By substitution, we can rewrite the functional as

$$\mathcal{F}^{\lambda}(\gamma) = \frac{1}{2}\int_0^L (k^2 + \lambda)\, ds = \frac{1}{2}\int_0^1 (k^2 + \lambda) v(t) dt.$$

The calculation involved is heavy and will not be included here. For the full calculation, please refer to [75]. The minimization of this functional depends on E, where

$$E = \frac{2k_{ss} + k^3 - \lambda k + 2Gk}{2} N.$$

Using the Frenet equations, the curve γ is an elastica provided that $E = 0$. In other words, γ is an elastica if and only if the following differential equation holds:

$$2k_{ss} + k^3 - \lambda k + 2Gk = 0.$$

By integrating, we get

$$k_s^2 + \frac{k^4}{4} + (G - \frac{\lambda}{2})k^2 = A.$$

Letting $u = k^2$, this becomes

$$u_s^2 + u^3 + 4(G - \frac{\lambda}{2})u^2 - 4Au = 0,$$

which has the following solutions:

1. $u = k^2 =$ constant, $\tau = 0$ which form only the circle and the straight line.

2. $k = k_0 \text{sech}(\frac{k_0}{2w}s)$, $\tau = 0$ which form borderline elastica.

3. $k = k_0 \text{cn}(\frac{k_0}{2w}s, p)$, $\tau = 0$ which form orbitlike elastica.

4. $k = k_0 \text{dn}(\frac{k_0}{2w}s, p)$, $\tau = 0$ which form wavelike elastica.

5. $k^2 = k_0^2(1 - \frac{p^2}{w^2}\text{sn}^2(\frac{k_0}{2w}s, p))$, where $4G - 2\lambda = \frac{k_0^2(1+p^2-3w^2}{w^2}$ and $0 \leq p \leq w \leq 1$.

4.4 The Minimum Variation Curve

The Minimum Variation Curve (MVC) is defined as the curve minimizing the arc-length integral of the variation of curvature,

$$\int_0^l \dot{k}^2 \, ds.$$

Introduced by Henry Moreton in 1992, he argued that the four-parameter MVC spline is a better alternative to the two-parameter MEC spline due to its limitations. For one, the MEC fails the roundness property. But because the MVC forms circular arcs naturally, a circular arc has zero curvature variation. Trivially, it is the curve that minimizes the MVC cost functional when the input points are co-circular [57], [64]. Second, the MVC is extensional, along with obtaining locality. Third, while the MEC tries to find the curve that bends the least, the MVC bends as smoothly (uniformly) as possible and is more stable to changes in shape [16]. Fourth, it is naturally convex preserving since it is guaranteed not to have any extraneous points of inflection [64]. Despite these advantages that the MVC has over the MEC, fairness is not captured by the minimization of the variation of curvature either.

Just like the MEC functional, the MVC functional can be explored via similar variational techniques. By using similar techniques, we arrive at the Euler-Lagrange equation of

$$E = \ddddot{k} + k^2\ddot{k} + \frac{1}{2}k\dot{k}^2 = 0.$$

Since solving fourth-order nonlinear differential equations are difficult (and perhaps impossible) to solve analytically, most presentations of this curve use a numerical approach to minimize the cost functional.

Chapter 5

A Proposed Energy Functional and Its Special Solutions

Note that in this chapter, we will use formulas from Byrd and Friedman's *Handbook of Elliptic Integrals for Scientists and Engineers*. We will refer to the appropriate formulas used in the calculations by "Byrd-Friedman", followed by the formula number as listed in the book.

5.1 The Derivation of the Euler-Lagrange Equation

Using similar techniques with the geometric approach to elastic curves in a previous chapter, we will need to find $W(k^2)$, $W(k^4)$ and $W(\dot{k}^2)$. We already know the formula for $W(k^2)$:

$$W(k^2) = 2k\langle \nabla_T^2 W, N\rangle + 2k\langle R(W,T)T, N\rangle + 4gk^2.$$

But since we are looking at this curve in $\mathbb{R}^2$, the curvature tensor $R(W,T)T = 0$, so this can be simplified to

$$W(k^2) = 2k\langle \nabla_T^2 W, N\rangle + 4gk^2$$

which is equivalent to

$$W(k^2) = 2\langle \nabla_T^2 W, kN\rangle + 4gk^2.$$

The derivation of $W(k^4)$ follows similarly

$$\begin{aligned} W(k^4) &= W(k^2 \cdot k^2) \\ &= k^2 W(k^2) + k^2 W(k^2) \\ &= 2k^2 W(k^2) \\ &= 2k^2(2\langle \nabla_T^2 W, kN\rangle + 4gk^2) \\ &= 4k^2\langle \nabla_T^2 W, kN\rangle + 8gk^4 \\ &= \langle \nabla_T^2 W, 4k^3 N\rangle + 8gk^4. \end{aligned}$$

The derivation of $W(\dot{k}^2)$ is exhaustive and for the purpose of this paper, will not be shown. All we need to know is that

$$W(\dot{k}^2) = 2\langle \nabla_T^3 W, \nabla_T^2 T\rangle - \langle \nabla_T^2 W, 4k^3 N\rangle - 2\ddot{g}k^2 + 6\dot{g}k\dot{k} + 6g\dot{k}^2 - 2gk^4$$

where $g = -\langle \nabla_T W, T\rangle$.

Next, we compute $\frac{d}{dw}\int \frac{1}{2}\dot{k}^2 - \frac{1}{8}k^4 \; ds$

$$
\begin{aligned}
\frac{d}{dw}\int \frac{1}{2}\dot{k}^2 - \frac{1}{8}k^4 \; ds &= \int \frac{1}{2}W(\dot{k}^2) - \frac{1}{8}W(k^4) \; ds \\
&= \int \langle \nabla_T W, J \rangle
\end{aligned}
$$

where $J = (\frac{3}{8}k^4 - \frac{1}{2}\dot{k}^2 + k\ddot{k})T + (\dddot{k} + \frac{3}{2}k^2\dot{k})N$. And so, the Euler-Lagrange equation for k is:

$$
E = \ddddot{k} + \frac{5}{2}k^2\ddot{k} + \frac{5}{2}k\dot{k}^2 + \frac{3}{8}k^5 = 0.
$$

Note that this equation actually looks *worse* than the MVC equation! However, it happens to be a completely integrable Hamiltonian equation (though that does not make it necessarily easy to integrate!) But we can at least reduce this Euler-Lagrange equation down to a third-order nonlinear differential equation by multiplying the entire equation by $-\dot{k}$ and doing the integration, i.e.

$$
H = -\dot{k}E = -\dddot{k}\dot{k} + \frac{1}{2}\ddot{k}^2 - \frac{5}{4}k^2\dot{k}^2 - \frac{1}{16}k^6.
$$

As mentioned back in Chapter 1, three special solutions of this functional are two elliptic curves of the form:

$$
k = A\mathrm{cn}(\alpha s, p) \text{ where } A = 2\alpha p
$$

where the elliptic modulus is

$$
p^2 = \frac{3-\sqrt{3}}{6} \text{ or } p^2 = \frac{3+\sqrt{3}}{6}
$$

and

$$k = \frac{1}{\wp(s; 0, \frac{1}{4})},$$

the Kiepert trefoil. We will now examine each solution separately.

5.2 The Elliptic Curve $k = A\text{cn}(\alpha s, p)$

Since we know some special solutions, we would like to know what their corresponding energies are. We do this by substituting each solution back into the functional $\mathcal{F} = \int \frac{1}{2}\dot{k}^2 - \frac{1}{8}k^4 \, ds$ and evaluate the integral. First we will look at the solution $k = A\text{cn}(\alpha s, p)$ where $A = 2\alpha p$ where the elliptic modulus is $p^2 = \frac{3-\sqrt{3}}{6}$ or $p^2 = \frac{3+\sqrt{3}}{6}$.

$$\begin{aligned}
\dot{k} &= -A\alpha \ \text{sn}(\alpha s, p)\text{dn}(\alpha s, p) \\
\dot{k}^2 &= A^2\alpha^2 \ \text{sn}^2(\alpha s, p)\text{dn}^2(\alpha s, p) \\
&= (2\alpha p)^2\alpha^2 \ \text{sn}^2(\alpha s, p)\text{dn}^2(\alpha s, p) \\
&= 4\alpha^4 p^2 \ \text{sn}^2(\alpha s, p)\text{dn}^2(\alpha s, p)
\end{aligned}$$

and

$$\begin{aligned}
k^4 &= A^4 \ \text{cn}^4(\alpha s, p) \\
&= (2\alpha p)^4 \ \text{cn}^4(\alpha s, p) \\
&= 16\alpha^4 p^4 \ \text{cn}^4(\alpha s, p).
\end{aligned}$$

Thus,

$$\int \frac{1}{2}\dot{k}^2 - \frac{1}{8}k^4 \; ds = \int \frac{1}{2}[4\alpha^4 p^2 \; \mathrm{sn}^2(\alpha s, p)\mathrm{dn}^2(\alpha s, p)] - \frac{1}{8}[16\alpha^4 p^4 \; \mathrm{cn}^4(\alpha s, p)] \; ds$$
$$= 2\alpha^4 p^2 \; \mathrm{sn}^2(\alpha s, p)\mathrm{dn}^2(\alpha s, p) - 2\alpha^4 p^4 \; \mathrm{cn}^4(\alpha s, p) \; ds$$
$$= 2\alpha^4 p^2 \int \mathrm{sn}^2(\alpha s, p)\mathrm{dn}^2(\alpha s, p) \; ds - 2\alpha^4 p^4 \int \mathrm{cn}^4(\alpha s, p) ds$$

From Byrd and Friedman (312.04) and (361.01), we know that

$$\int \mathrm{cn}^4 u \; du = \frac{1}{3k^4}[(2-3k^2)k'^2 u + 2(k^2-1)E(u) + k^2 \mathrm{sn}u \; \mathrm{cn}u \; \mathrm{dn}u]$$
$$\int \mathrm{sn}^2 u \; \mathrm{dn}^2 u \; du = \frac{1}{3k^2}[(2k^2-1)E(u) + k'^2 u - k^2 \mathrm{sn}u \; \mathrm{cn}u \; \mathrm{dn}u]$$

where

$k =$ modulus of the Jacobian elliptic functions and integrals

$E(u) = E(\phi, k) =$ Legendre's incomplete elliptic integral of the second kind, $\phi = \mathrm{am}u$

$k' =$ the complementary modulus $= \sqrt{1-k^2}$.

To alleviate confusion between the curvature and the elliptic modulus, we will replace the elliptic modulus in the Byrd-Friedman definition k with p.

Using variable substitution from elementary calculus with $u = \alpha s$ and $\frac{1}{\alpha} \; du = ds$, we get that

$$\int \mathrm{sn}^2(\alpha s, p)\mathrm{dn}^2(\alpha s, p)\ ds = \frac{1}{\alpha}\int \mathrm{sn}^2(u,p)\mathrm{dn}^2(u,p)\ ds$$
$$= \frac{1}{3\alpha p^2}[(2p^2-1)E(\alpha s) + p'^2(\alpha s) - p^2\mathrm{sn}(\alpha s, p)\mathrm{cn}(\alpha s, p)\mathrm{dn}(\alpha s, p)]$$

$$\int \mathrm{cn}^4(\alpha s, p)ds = \frac{1}{\alpha}\int \mathrm{cn}^4(u,p)ds$$
$$= \frac{1}{3\alpha p^4}[(2-3p^2)p'^2(\alpha s) + 2(p^2-1)E(\alpha s) + p^2\mathrm{sn}(\alpha s, p)\ \mathrm{cn}(\alpha s, p)\ \mathrm{dn}(\alpha s, p)]$$

where $E(\alpha s) = E(\phi, p) = \int_0^\phi \sqrt{1 - p^2\sin^2\theta}\ d\theta$.

Putting all of the above together, we get that

$$\int \frac{1}{2}\dot{k}^2 - \frac{1}{8}k^4\ ds = \frac{2}{3}\alpha^3[2p^2-1)E(\alpha s) + (1-p^2)(\alpha s) - p^2\mathrm{sn}(\alpha s, p)\mathrm{cn}(\alpha s, p)\mathrm{dn}(\alpha s, p)]$$
$$-\frac{2}{3}\alpha^3[(2-3p^2)(1-p^2)(\alpha s) + 2(p^2-1)E(\alpha s) + p^2\mathrm{sn}(\alpha s, p)\ \mathrm{cn}(\alpha s, p)\ \mathrm{dn}(\alpha s, p)]$$
$$= -2\alpha^3 E(\alpha s) - \frac{4}{3}\alpha^3 p^2\mathrm{sn}(\alpha s, p)\ \mathrm{cn}(\alpha s, p)\ \mathrm{dn}(\alpha s, p) + \alpha^4 s\Big(-2p^4 + \frac{8}{3}p^2 - \frac{2}{3}\Big)$$

To find the total energy, we will need to evaluate the integral from $s = 0$ to $s = \frac{K}{\alpha}$.
This yields
$$-2\alpha^3 E(p) + \alpha^3 K(p)\Big(-2p^4 + \frac{8}{3}p^2 - \frac{2}{3}\Big).$$

We will focus on the derivation of the first portion of the total energy integral since that has a significant importance to the research. From properties of the Jacobi elliptic integral and its special values at K and 0 discussed in Byrd-Friedman (122.01) and (122.02), we get:

$$\begin{aligned}
\int_0^{\frac{K}{\alpha}} \frac{1}{2}\dot{k}^2\, ds &= \frac{2}{3}\alpha^3[(2p^2-1)E(\alpha s) + (1-p^2)(\alpha s) - p^2\mathrm{sn}(\alpha s,p)\mathrm{cn}(\alpha s,p)\mathrm{dn}(\alpha s,p)]\Big|_0^{\frac{K}{\alpha}} \\
&= \frac{2}{3}\alpha^3[(2p^2-1)E(K) + (1-p^2)(K) - p^2\mathrm{sn}(K,p)\mathrm{cn}(K,p)\mathrm{dn}(K,p)] \\
&- \frac{2}{3}\alpha^3[(2p^2-1)E(0) + (1-p^2)(0) - p^2\mathrm{sn}(0,p)\mathrm{cn}(0,p)\mathrm{dn}(0,p) \\
&= \frac{2}{3}\alpha^3[(2p^2-1)E(K) + (1-p^2)(K) - p^2\cdot 1\cdot 0\cdot\sqrt{1-p^2} \\
&- \frac{2}{3}\alpha^3\Big[(2p^2-1)\cdot\frac{\pi}{2} + 0 - p^2\cdot 0\cdot 1\cdot 1\Big] \\
&= \frac{2}{3}\Big[(2p^2-1)E(K) + (1-p^2)(K)\Big] - \frac{2}{3}\alpha^3\Big[\frac{\pi}{2}(2p^2-1)\Big] \\
&= \frac{2}{3}\alpha^3\Big[(2p^2-1)E(K) + (1-p^2)(K) - \frac{\pi}{2}\Big(2p^2-1\Big)\Big]
\end{aligned}$$

We have two cases to consider since we have two moduli. For the case when $p^2 = \frac{3-\sqrt{3}}{6}$, we have

$$\int_0^{\frac{K}{\alpha}} \frac{1}{2}\dot{k}^2\, ds \approx 0.0643194\ \alpha^3.$$

For the case when $p^2 = \frac{3+\sqrt{3}}{6}$, we have

$$\int_0^{\frac{K}{\alpha}} \frac{1}{2}\dot{k}^2\, ds \approx 0.608067\ \alpha^3.$$

We can do the same with the other functional. Similarly from properties of the Jacobi elliptic integral and its special values at K and 0 discussed in Byrd-Friedman (122.01) and (122.02), we get:

$$\begin{aligned}
\int_0^{\frac{K}{\alpha}} \frac{1}{8}k^4\, ds &= \frac{2}{3}\alpha^3[(2-3p^2)(1-p^2)(\alpha s) + 2(p^2-1)E(\alpha s) + p^2 \mathrm{sn}(\alpha s,p)\mathrm{cn}(\alpha s,p)\mathrm{dn}(\alpha s,p)]\Big|_0^{\frac{K}{\alpha}} \\
&= \frac{2}{3}\alpha^3[(2-3p^2)(1-p^2)(K) + 2(p^2-1)E(K) + p^2\mathrm{sn}(K,p)\mathrm{cn}(K,p)\mathrm{dn}(K,p)] \\
&- \frac{2}{3}\alpha^3[(2-3p^2)(1-p^2)(0) + 2(p^2-1)E(0) + p^2\mathrm{sn}(0,p)\mathrm{cn}(0,p)\mathrm{dn}(0,p)] \\
&= \frac{2}{3}\alpha^3\left[(2-3p^2)(1-p^2)(K) + 2(p^2-1)E(K) + p^2\cdot 1\cdot 0\cdot\sqrt{1-p^2}\right] \\
&- \frac{2}{3}\alpha^3\left[2(p^2-1)\cdot\frac{\pi}{2} + p^2\cdot 0\cdot 1\cdot 1\right] \\
&= \frac{2}{3}\alpha^3[(2-3p^2)(1-p^2)(K) + 2(p^2-1)E(K)] - \frac{2}{3}\alpha^3[\pi(p^2-1)] \\
&= \frac{2}{3}\alpha^3[(2-3p^2)(1-p^2)(K) + 2(p^2-1)E(K) - \pi(p^2-1)]
\end{aligned}$$

We will leave the details of the evaluation to the reader. By combining both results, we achieve the total energy of the overall functional for both moduli. For $p^2 = \frac{3-\sqrt{3}}{6}$, we have

$$\int \frac{1}{2}\dot{k}^2 - \frac{1}{8}k^4\, ds \approx 0.0619257\ \alpha^3$$

and for $p^2 = \frac{3+\sqrt{3}}{6}$, we have

$$\int \frac{1}{2}\dot{k}^2 - \frac{1}{8}k^4\, ds \approx 0.111752\ \alpha^3.$$

Based on these calculations, we can say that the functional will be minimized when the modulus is $p^2 = \frac{3-\sqrt{3}}{6}$.

5.3 An Analysis of the Jacobi Elliptic Function Solutions

While we know the values of the change in curvature and the total energy of the Jacobi elliptic functions, we do not know what their corresponding curves look like. In other words, we know the curvature of these special solutions but we do not know what the actual curves corresponding to these solutions look like. We can find these curves by appealing to the *Fundamental Theorem of Curves*.

The Fundamental Theorem of Curves states that a curve is completely determined by the curvature and torsion, up to isometry. However, trying to solve the Frenet frame system of differential equations is difficult in general. The good news is that with planar curves (where the torsion is zero), is is possible to find an integral formula for the curve coordinates in terms of the curvature. In turn, we can figure out that the x- and y-coordinates of the curve parametrization will be. These formulas are called the *natural equations*, which specifies a curve independent of any choice of coordinates or parametrization. We will not bother with the minute details but all we need to do is to solve for the following:

$$\theta(s) = \int k \; ds \qquad x(s) = \int \cos(\theta) \; ds \qquad y(s) = \int \sin(\theta) \; ds.$$

For $k = 2\alpha p \operatorname{cn}(\alpha s, p)$, we find θ by integrating k:

$$\theta(s) = \int k \; ds = \frac{2p \arccos(\operatorname{dn}(\alpha s, p)) \operatorname{sn}(\alpha s, p)}{\sqrt{1 - \operatorname{dn}(\alpha s, p)^2}}.$$

But by Byrd-Friedman (121.00), $\theta(s)$ can be simplified by the identity $p \operatorname{sn}(\alpha s, p) =$

$\sqrt{1-\mathrm{dn}(\alpha s,p)^2}$:

$$\theta(s) = \int k\ ds = \frac{2p\arccos(\mathrm{dn}(\alpha s,p))\,\mathrm{sn}(\alpha s,p)}{p\,\mathrm{sn}(\alpha s,p)} = 2\arccos(\mathrm{dn}(\alpha s,p).$$

Since we now know θ, we can find the x- and y-coordinates of the curve parametrization:

$$x(s) = \int \cos(2\arccos(\mathrm{dn}(\alpha s,p))\ ds \quad y(s) = \int \sin(2\arccos(\mathrm{dn}(\alpha s,p))\ ds.$$

While the formulas for the x- and y-coordinates are messy, there is a property involving sine, cosine and inverse cosine inputs which will simplify it considerably:

$$\cos(2\arccos(f(x)) = 2f(x)^2 - 1$$
$$\sin(2\arccos(f(x)) = 2f(x)\sqrt{1-f(x)^2}.$$

With these identities, we can simplify $x(s)$ and $y(s)$ as

$$x(s) = \int \cos(2\arccos(\mathrm{dn}(\alpha s,p))\ ds = \int 2\mathrm{dn}(\alpha s,p)^2 - 1\ ds$$
$$y(s) = \int \sin(2\arccos(\mathrm{dn}(\alpha s,p))\ ds = \int 2\mathrm{dn}(\alpha s,p)\sqrt{1-\mathrm{dn}(\alpha s,p)^2}\ ds.$$

Now using the identity Byrd-Friedman (121.00) mentioned above and integrating the functions by using Byrd-Friedman (121.00), (314.02) and (360.02), we get our parametrized curve $(x(s), y(s))$ where

$$x(s) = \int 2\mathrm{dn}(\alpha s, p)^2 - 1 \; ds = \frac{2E(am(\alpha s, p), p)}{\alpha s} - s$$
$$y(s) = \int 2\mathrm{dn}(\alpha s, p)\sqrt{1 - \mathrm{dn}(\alpha s, p)^2} \; ds = -\frac{2p\,\mathrm{cn}(\alpha s, p)}{\alpha}.$$

5.4 The Trefoil $k = \frac{1}{\wp(\sqrt{2}s;\, 0,\, \frac{1}{8})}$

Another special to the minimization of our functional is the curve which has a curvature of $\frac{1}{\wp(\sqrt{2}s; 0, \frac{1}{8})}$. The corresponding curve to this curvature is the Kiepert trefoil, which is a sextic curve that can be represented in polar coordinates by

$$r^3 = 2\cos(3\theta)$$

and in Cartesian coordinates by

$$(x^2 + y^2)^3 = 2x^3 - 6xy^2.$$

By using isotropic coordinates of $R = x + iy$ and $B = x - iy$, the Cartesian form can be rewritten as

$$R^3B^3 = R^3 + B^3.$$

As noted in various sources ([50], [53], [55]), the trefoil has a multitude of fascinating properties. For one, in [53], the arc-length parametrization is given by rational expressions in the elliptic function ϕ and its derivative, where ϕ is the solution of the differential equation

$$\left(\frac{d\phi}{dt}\right)^2 = 1 - \phi(t)^3, \quad \text{where} \quad \phi(0) = 0.$$

The arc-length parametrization of the trefoil can be expressed in terms of Dixon elliptic functions. This is unusual since for no other elliptic curve of low degree ($d < 8$) can be so parametrized by elliptic functions [55].

By using the formulas in [53], the following facts can be derived:

Proposition 5.4.1

1. *The curvature k of the trefoil satisfies the equation $k = 2r^2$.*

2. *The curvature satisfies the differential equation*

$$\left(\frac{dk}{ds}\right)^2 + \frac{1}{4}k^4 = 8k.$$

3. $k(s) = 1/\wp(\sqrt{2}s; 0, 1/8)$, *where $\wp$ is the Weierstrass $\wp$-function.*

Proof . We will refrain from the whole proof and just provide a sketch of the details. We will use the Dixon elliptic functions $S = \mathrm{sm}(is)$ and $C = \mathrm{cm}(is)$. Recall that $S^3 + C^3 = 1$, $S' = iC^2$ and $C' = -iS^2$. The parametrized trefoil is given by arc-length parametrization

$$x(s) = \frac{S}{2} - \frac{S}{2C}, \qquad y(s) = \frac{S}{2i} + \frac{S}{2iC}.$$

By direct calculation, we find that

$$x^2 + y^2 = -\frac{S^2}{C} \qquad \text{and} \qquad k = -\frac{2S^2}{C}.$$

The function $-\frac{2S^2}{C}$ satisfies the differential equation, as does the Weierstrass function, and they both vanish at 0. ∎

As with the Jacobi elliptic functions in the previous section, we would like to know the corresponding energy to our Weierstrass elliptic function. We could use the same technique as we did with the analysis with the Jacobi elliptic functions, substitute $k = \dfrac{1}{\wp(\sqrt{2}s; 0, \frac{1}{8})}$ into the functional and use Byrd-Friedman formulas to evaluate. However, the derivation is extremely long and will not be included here. Instead, we will utilize a few facts we know about the trefoil to derive a more compact and elegant answer.

Since we know that the curvature k of the trefoil satisfies the differential equation $\left(\dfrac{dk}{ds}\right)^2 + \dfrac{1}{4}k^4 = 8k$, we can derive the following facts:

$$\dot{k}^2 = 8k - \frac{1}{4}k^4 \quad \text{and} \quad \ddot{k} = 4 - \frac{1}{2}k^3.$$

This leads to

$$\frac{d(k\dot{k})}{ds} = k\ddot{k} + \dot{k}^2 = 12k - \frac{3}{4}k^4.$$

Therefore, by putting these pieces together, we get

$$\int \frac{1}{2}\dot{k}^2 - \frac{1}{8}k^4 \, ds = \int 4k - \frac{1}{4}k^4 \, ds = \int \frac{1}{3}\frac{d(k\dot{k})}{ds} \, ds = \frac{1}{3}k\dot{k} + C.$$

This result actually leads to a simple, yet elegant and remarkable discovery about the trefoil:

Theorem 5.4.2

The total energy of the trefoil defined as $\int \frac{1}{2}\dot{k}^2 - \frac{1}{8}k^4 \, ds$ over a half leaf (from the *origin to the end of the leaf) is zero. In particular, the total energy of the entire trefoil is zero.*

Proof .

Take the polar equation of the trefoil $r^3 = 2\cos(3\theta)$. We know this curve will achieve its maximum when $\cos(3\theta) = 1$, i.e. $\theta = \frac{2n\pi}{3}$ where $n \in \mathbb{Z}$. This implies that at maximum, $r^3 = 2$ which corresponds to a polar radius $r = \sqrt[3]{2}$. This can be rewritten in Cartesian coordinates as $r^2 = x^2 + y^2 = \sqrt[3]{4}$. And so, at the intersection of the trefoil with Cartesian form $(x^2 + y^2)^3 = 2x^3 - 6xy^2$ and the circle where the maxima occur, we get three points which all lie on the tip of each leaf (See Figure 5.1):

$$A = \Big(-\frac{1}{\sqrt[3]{4}}, \frac{\sqrt{3}}{\sqrt[3]{4}}\Big), \quad B = \Big(-\frac{1}{\sqrt[3]{4}}, -\frac{\sqrt{3}}{\sqrt[3]{4}}\Big), \quad \text{and} \quad C = (\sqrt[3]{2}, 0),$$

all of which have a polar radius of $r = \sqrt[3]{2}$

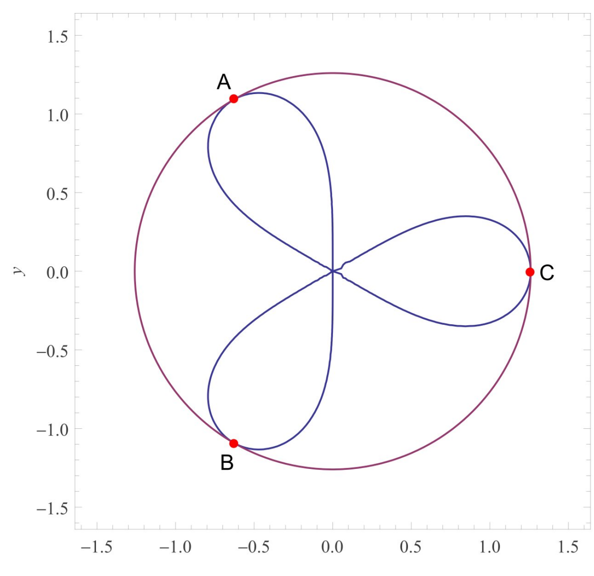

Figure 5.1: Maxima on the trefoil

We know that the total energy of the trefoil is given by

$$\int \frac{1}{2}\dot{k}^2 - \frac{1}{8}k^4 \, ds = \frac{1}{3}k\dot{k} + C.$$

Since $k = 2r^2$ and $\dot{k} = 2r\sqrt{4 - r^6}$, we know that at the origin ($r = 0$) and at the end of the leaf ($r = \sqrt[3]{2}$), $k\dot{k} = 0$. Thus, it follows that the energy of a half leaf is zero. In particular, this means the energy of a whole leaf is also zero and so must the energy of the entire trefoil as well.

∎

Using Mathematica, the half-periods of the Weierstrass elliptic function $\wp(\sqrt{2}s; 0; \frac{1}{8})$ that gives us the curvature of the trefoil are

$$\omega_1 = \frac{e^{\frac{i\pi}{3}}\Gamma(\frac{1}{3})^3}{4\pi} \qquad \text{and} \qquad \omega_2 = \frac{\Gamma(\frac{1}{3})^3}{4\pi},$$

where Γ is the *gamma function*.

Since most of the literature involve minimizing the integral of the change of curvature, we would like to evaluate for it over the real half-period. The real half-period exposes a "linear system" relationship between the total energy integral and the individual integrands:

$$\int_0^{\omega_2} \frac{1}{2}\dot{k}^2 \, ds - \int_0^{\omega_2} \frac{1}{8}k^4 \, ds = 0$$
$$\int_0^{\omega_2} \frac{1}{2}\dot{k}^2 \, ds + \int_0^{\omega_2} \frac{1}{8}k^4 \, ds = 4\int_0^{\omega_2} k \, ds$$

This implies that

$$\frac{1}{2}\int_0^{\omega_2} \dot{k}^2 \, ds = 2\int_0^{\omega_2} k \, ds.$$

Note the integral on the right hand side. This is actually the *total curvature* over one-sixth of the length of the trefoil. The total curvature over a closed interval measures the rotation of the unit tangent vector as the parameter s changes over the interval. For a closed curve, the total curvature is always an integer multiple of 2π and for the trefoil, its total curvature is 4π. But since we are only looking at one-sixth of the curve based on the bounds, we get a value of $\frac{4\pi}{6}$. If we double this value, we get the value of the change of curvature along the interval $[0, \omega_2]$, which is $\frac{4\pi}{3}$:

$$\frac{1}{2}\int_0^{\omega_2} \dot{k}^2 \, ds = 2\int_0^{\omega_2} k \, ds = 2 \cdot \frac{4\pi}{6} = \frac{4\pi}{3}.$$

5.5 Scale-Invariant Minimization of Our Special Solutions

So far, we have seen the numerical values of the total energy and the change of curvature for each of the special solutions we have found for minimizing the functional $\int \frac{1}{2}\dot{k}^2 - \frac{1}{8}k^4 \;\; ds$. We see that by looking at total energy, the trefoil $k = \dfrac{1}{\wp(\sqrt{2}s; 0, \frac{1}{8})}$ is the more attractive choice. But by looking at the change of curvature, the Jacobi function $k = A\mathrm{cn}(\alpha s, p)$, where $p^2 = \frac{3-\sqrt{3}}{6}$ is the better one. In the current literature about curve minimization, the proposed desirable metric for fairness is the integral of the change of curvature (called the MVC). We would like to see how the MVC compare to all the special solutions we have found.

However, the integral of the change of curvature (called the MVC) is not without its problems. While the shape of the curve is independent of scaling, the value of its functional is decreased when its defining geometric constraints are scaled up [73]. There are cases where this integral can become unstable. This happens whenever the curve in question has an inflection point between constraints and turns too large an angle [65]. The instability is also caused by a reduction in the value of the functional as the scaling of the curve increases. As the arc length of the curve grows linearly, its derivative decreases reciprocally. For example, the MVC decreases in proportion to the cube of the arc length [73]. To offset these run-away tendencies, Moreton and Séquin proposed a scale-invariant version of the MVC (abbreviated as SI-MVC). This is done by multiplying the minimizing integral by a factor that increases with the scale factor, the arc length. For the case of the MVC, to counteract its growth tendency, we multiply by the cube of the arc length. This tweak keeps the desirable properties of the MVC and makes the integral more stable [65].

But why does this make sense? Let's take a look at a simple example. Suppose $y = 1 - x^2$ and we would like to take to integral the change of curvature over the arc length between the points $(0,1)$ and $(1,0)$. Then:

$$
\begin{aligned}
k &= \frac{-2}{(1+4x^2)^{3/2}} \\
\dot{k} &= \frac{dk}{ds} = \frac{dk}{dx}\frac{dx}{ds} \qquad \text{where} \qquad \frac{dx}{ds} = \frac{1}{\sqrt{1+y'^2}} \\
&= \frac{24x}{(4x^2+1)^{5/2}} \cdot \frac{1}{\sqrt{4x^2+1}} \\
&= \frac{24x}{(4x^2+1)^3} \\
\frac{1}{2}\dot{k}^2 &= \frac{288x^2}{(4x^2+1)^6}
\end{aligned}
$$

With this information, we can start forming the integral

$$\int_0^1 \frac{1}{2}\dot{k}^2\ ds = \int_0^1 \frac{288x^2}{(4x^2+1)^{5/2}}\ dx.$$

By letting $x = \frac{1}{2}\tan\theta$ and $dx = \frac{1}{2}\sec^2\theta$,

$$\int_0^1 \frac{1}{2}\dot{k}^2\ ds = \int_0^{\arctan(2)} \frac{36\tan^2\theta\sec^2\theta}{(\tan^2\theta+1)^{5/2}}\ d\theta.$$

But what would happen if we scale the endpoints of the arc length by t, i.e. $(0,t)$ and $(t,0)$? The equation of our curve would then become $y = t - \frac{x^2}{t}$ and we can derive the following:

$$\begin{aligned} k &= \frac{-2t^2}{(t^2+4x^2)^{3/2}} \\ \dot{k} &= \frac{dk}{ds} = \frac{dk}{dx}\cdot\frac{dx}{ds} = \frac{24xt^2}{(4x^2+t^2)^{5/2}}\cdot\frac{1}{\sqrt{\frac{4x^2}{t^2}+1}} = \frac{24xt^3}{(4x^2+t^2)^3} \\ \frac{1}{2}\dot{k}^2 &= \frac{288x^2t^6}{(4x^2+t^2)^6} \end{aligned}$$

We construct the integral

$$\int_0^t \frac{1}{2}\dot{k}^2\ ds = \int_0^t \frac{288x^2t^5}{(4x^2+t^2)^{5/2}}\ dx.$$

By letting $x = \frac{t}{2}\tan\theta$ and $dx = \frac{t}{2}\sec^2\theta$ and with some clever algebraic manipulation, we get

$$\int_0^t \frac{1}{2}\dot{k}^2\ ds = \frac{1}{t^3}\int_0^{\arctan(2)} \frac{36\tan^2\theta\sec^2\theta}{(\tan^2\theta+1)^{5/2}}\ d\theta.$$

As we can see, by scaling the arc length by t, the MVC functional decreases in proportion by a cube.

We will begin by finding the arc length for each of the curves. For each of the Jacobi functions, the y-coordinate $-\frac{2p\,\mathrm{cn}(\alpha s,p)}{\alpha}$ will be zero at the points where the graph meets the x-axis. Since the y-coordinate is the Jacobi cosine function scaled by a constant, we will need to find where that Jacobi cosine function is zero. By Byrd and Friedman, the y-coordinate will be zero whenever the argument is the quarter-period K, where K is the complete elliptic integral of the first kind, i.e. $K = F(\frac{\pi}{2}, p)$. Also, due to the doubly periodic behavior of the function, the Jacobi cosine function will also be zero whenever the argument is $(2n+1)K$, where n is an integer. In other words,

$$-\frac{2p\,\mathrm{cn}(\alpha s,p)}{\alpha} = 0 \qquad \text{whenever} \qquad s = \frac{(2n+1)K}{\alpha}.$$

For each of the cases for the elliptic parameter p^2, we will calculate the arc length of the curve as we go from $s = \frac{K}{\alpha}$ to $\frac{5K}{\alpha}$ since it appears to be periodic every $4K$. For $p^2 = \frac{3-\sqrt{3}}{6}$, $E \approx 1.66538$ and the arc length is approximately $\frac{6.66152}{\alpha}$. Likewise, for $p^2 = \frac{3+\sqrt{3}}{6}$, $E \approx 2.23222$ and the arc length is approximately $\frac{8.92888}{\alpha}$. All of these values were computed using Mathematica.

For the trefoil $r^3 = 2\cos(3\theta)$, we will calculate the arc length of one-sixth of the trefoil. We will integrate from $\theta = 0$ to $\theta = \alpha$, where α is the smallest positive number for which $2\cos(3\theta) = 0$. This gives $\alpha = \frac{\pi}{6}$. Since the equation for the trefoil is in polar form, the arc length is given by

$$L = \int_0^{\frac{\pi}{6}} \sqrt{r^2 + \left(\frac{dr}{d\theta}\right)^2}\, d\theta.$$

Starting with $r^3 = 2\cos(3\theta)$,

$$3r^2 \frac{dr}{d\theta} = -6\sin(3\theta)$$
$$\frac{dr}{d\theta} = \frac{-2\sin(3\theta)}{(2\cos(3\theta))^{2/3}}$$
$$\left(\frac{dr}{d\theta}\right)^2 = \frac{\sqrt[3]{4}\sin^2(3\theta)}{(\cos(3\theta))^{4/3}}$$
$$r^2 + \left(\frac{dr}{d\theta}\right)^2 = \frac{\sqrt[3]{16}\sin^2(3\theta)}{(\cos(3\theta))^{2/3}}$$

And so,

$$L = \int_0^{\frac{\pi}{6}} \sqrt{\frac{\sqrt[3]{16}\sin^2(3\theta)}{(\cos(3\theta))^{2/3}}}\, d\theta = \frac{\sqrt[3]{4}}{2} \approx 0.793700526$$

Since we now calculated the arc lengths of these special solutions, we can compare the values of the scale-invariant MVC of each one. These values are displayed on the table below:

Table 5.1: Various Energies of the Special Solutions

Curve	**Arc Length** **L**	**MVC** $\frac{1}{2}\int \dot{k}^2\, ds$	**SI-MVC** $\frac{1}{2}L^3 \int \dot{k}^2\, ds$	**Total Energy** $\int \frac{1}{2}\dot{k}^2 - \frac{1}{8}k^4\, ds$
Jacobi, $p^2 = \frac{3-\sqrt{3}}{6}$	$6.66152/\alpha$	$0.0643194\alpha^3$	19.01349666	$0.0619257\alpha^3$
Jacobi, $p^2 = \frac{3+\sqrt{3}}{6}$	$8.92888/\alpha$	$0.608067\alpha^3$	432.8549552	$0.111752\alpha^3$
Trefoil	0.793700526	4.18879	2.094395102	0

But notice that when we calculate the SI-MVC for these special solutions, we get that the trefoil is actually the more desirable curve since it has the lowest energy.

5.6 Other Analytical Solutions

A major problem with nonlinear differential equations is that they lack a superposition principle. For linear differential equations, if we know two solutions $f(x)$ and $g(x)$, then so is their linear combination $af(x) \pm bg(x)$, where a, b are arbitrary constants.

But this does not work when dealing with nonlinear terms. So in general, the superposition is not a solution for nonlinear differential equations. A claim by Khare and Saxena declares that if $\mathrm{cn}(x, m)$ and $\mathrm{dn}(x, m)$ are solutions to a nonlinear differential equation, then so is their sum and difference, i.e. $\mathrm{dn}(x, m) \pm \sqrt{m}\mathrm{cn}(x, m)$. The authors do not provide a rigorous proof for this claim but by a number of examples, they have shown that a form a superposition does hold in the nonlinear case. They believe that this superposition principle holds possibly because both $\mathrm{cn}(x, m)$ and $\mathrm{dn}(x, m)$ are similar. By similar, both are even functions and both have identical derivatives when $m = 1$ since:

$$\frac{d}{dx}\mathrm{cn}(x, 1) = \frac{d}{dx}\mathrm{sech}(x) = -\tanh(x)\mathrm{sech}(x) = \frac{d}{dx}\mathrm{sech}(x) = \frac{d}{dx}\mathrm{dn}(x, 1).$$

This is in contrast to the Jacobi elliptic sine function, which is an odd function and when $m = 1$, $\mathrm{sn}(x, m) = \mathrm{sn}(x, 1) = \tanh(x)$. This is why the authors propose why superpositions of the form $\mathrm{cn}(x, m) + \mathrm{sn}(x, m)$ do not generally work in the examples they presented [44].

In terms of the differential equation we are working on, it can be shown that our two Jacobi cosine functions can also be expressed as Jacobi delta functions by means of a transformation noted in Byrd and Friedman. With that, the proposition applies and we can find additional solutions, if any exist. By supposing that there exists a solution in the form $k(s) = \mathrm{dn}(s, m) \pm \sqrt{m}\mathrm{cn}(s, m)$ and substituting that into the differential equation, we get:

$$\frac{1}{8}(3 + 2m + 3m^2)(\sqrt{m}\mathrm{cn}(s, m) + \mathrm{dn}(s, m)) = 0.$$

By solving the quadratic factor, we get that the proposed solution will make our differential equation vanish when $m = \frac{1}{3}(-1 \pm 2i\sqrt{2})$. The good news is that we have four new solutions but they are all of complex moduli:

$$k(s) = \mathrm{dn}(s, \frac{1}{3}(-1 + 2i\sqrt{2})) \pm \sqrt{\frac{1}{3}(-1 + 2i\sqrt{2})}\,\mathrm{cn}(s, \frac{1}{3}(-1 + 2i\sqrt{2}))$$

and

$$k(s) = \mathrm{dn}(s, \frac{1}{3}(-1 - 2i\sqrt{2})) \pm \sqrt{\frac{1}{3}(-1 - 2i\sqrt{2})}\,\mathrm{cn}(s, \frac{1}{3}(-1 - 2i\sqrt{2})).$$

But are these truly "new" solutions? There exists transformations where the modulus is purely imaginary in Byrd and Friedman. But according to the NIST Digital Library of Mathematical Functions, all of the transformations for Jacobi ellitpic functions are valid for all complex values of the moduli [66]. However, through examination, it appears that no transformation used produces the other two real solutions previously found. So, it is reasonable to believe that these four solutions, while having complex moduli, are indeed new solutions.

Chapter 6

The Trefoil as a Suitable Spline

6.1 A Comment on Aberrancy

Recall from Theorem 3.2.2 that a more geometric proof was presented as to how and why the quantity $\dot{k}/k^2$ is key to Levien's proof. The quantity $\dot{k}/k^2$ actually has a geometric interpretation that has been known since the 1800s but has received little to no attention. In fact, the last known textbook to discuss this concept was published in the turn of the twentieth century [71]. But interest in the concept re-emerged in 1978 by Schot's analysis on the geometry of the third derivative. This interpretation is called the *déviation* of a curve, or is better known as the *aberrancy* of a curve. Geometrically, the *aberrancy* of a curve $f(x)$ at a point P is the tangent of the angle δ formed between the normal at P and the limiting position of a line drawn from P to the midpoint of a chord parallel to the tangent line at P as the chord approaches P [71].

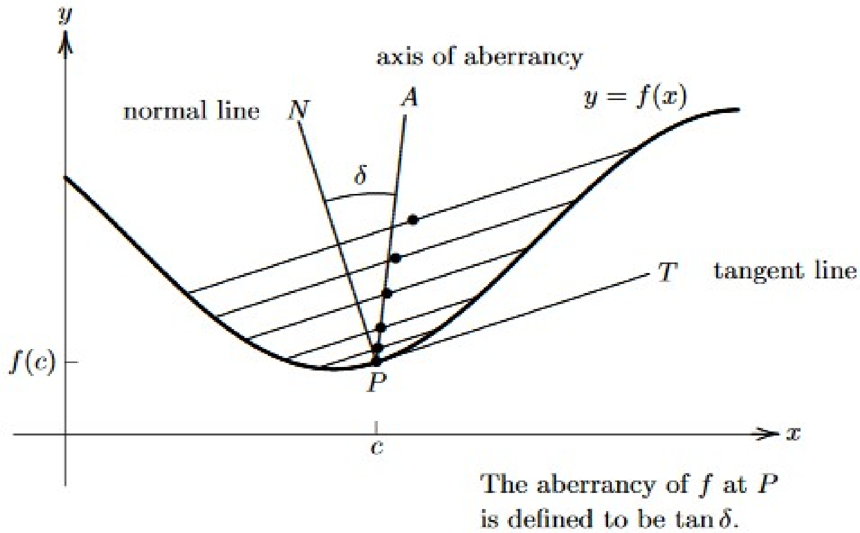

Figure 6.1: The aberrancy of a curve $f(x)$ at point P. Reprinted from [14].

For example, the circle has its tangent lines perpendicular to all its radii and so the parallel chords to a tangent line, at any given point, are also perpendicular to the radius. Then it follows that all midpoints in the chords lie on a perpendicular line to the tangent line since circles are curved away from a point equidistant to both sides. Hence, the line formed by these midpoints goes to the center of the circle and lies on the corresponding normal line. Therefore, the angle δ formed between the normal to the circle and the limiting line at any point is 0, which implies $\tan 0 = 0$. And so the aberrancy of the circle at any given point is 0. Any deviation from a circle will produce a non-zero aberrancy. With that, aberrancy can be thought of as the measure of the noncircularity of a curve at a given point [34].

The aberrancy of a curve can be represented as a formula. Suppose that $f(x)$ is a thrice-differentiable plane curve on an open interval I. If $c \in I$ and $f''(c) \neq 0$, then the *aberrancy* $A(c)$ of $f(x)$ at c is given by:

$$A(c) = f'(c) - \frac{f'''(c)(1 + f'(c)^2)}{3f''(c)^2} = \frac{1}{3}\frac{d\rho}{ds} = -\frac{1}{3}\frac{\dot{k}}{k^2},$$

where

$$\rho = \frac{1}{k} \text{ is the radius of curvature.}$$

We will note a few remarks. Aberrancy is invariant under both translation and rotation. The only curves with constant aberrancy are logarithmic spirals, where its intrinsic equation is $k = \frac{1}{bs}$. By doing the computation work, we arrive at $A(c) = -\frac{b}{3}$.

6.2 Candidates for Suitable Splines

As stated by Levien and rigorously shown in Theorem 3.2.2, the monotonicity of the quantity $\dot{k}/k^2$ plays an important role in determine which curves make suitable splines. This quantity represents the amount of curvature variation for a segment of a set amount of curvature. Meaning, it is invariant of similarity transformations including uniform scaling. So, for any given generator curve, it uniquely identifies a point on the curve (modulo periodicity, if the curve is periodic as opposed to monotone in curvature) [57]. Based on this condition Levien established, it can be shown that the solution curves from the minimization of the energy function $\int \frac{1}{2}\dot{k}^2 - \frac{1}{8}k^4 \, ds$ are candidates in making suitable splines.

For the trefoil, we know that its curvature satisfies the condition $\dot{k}^2 + \frac{1}{4}k^4 = 8k$.

Thus

$$\dot{k}^2 = -\frac{1}{4}k^4 + 8k.$$

By taking the derivative with respect to s on both sides, we get

$$\ddot{k} = -\frac{1}{2}k^3 + 4.$$

This implies

$$k^2\ddot{k} = -\frac{1}{2}k^5 + 4k^2 \quad \text{and} \quad 2k\dot{k}^2 = -\frac{1}{2}k^5 + 16k^2$$

which yields

$$k^2\ddot{k} - 2k\dot{k}^2 = -12k^2 < 0.$$

Thus, for the trefoil, the quantity $\dot{k}/k^2$ is monotonic.

For the other two solution curves which are elastic curves that have a curvature of $k = A\text{cn}(\alpha s, p)$ where $A = 2\alpha p$ and $p^2 = \dfrac{3 \pm \sqrt{3}}{6}$, it has a derivative of $\dot{k} = -A\alpha\text{sn}(\alpha s, p)\text{dn}(\alpha s, p)$ and a second derivative of $\ddot{k} = A\alpha^2\text{cn}(\alpha s, p)(p\text{sn}(\alpha s, p)^2 - \text{dn}(\alpha s, p)^2)$. And so, by substitution and simplification, we get

$$\frac{d}{ds}\left(\frac{\dot{k}}{k^2}\right) = \frac{k^2\ddot{k} - 2k\dot{k}^2}{k^4} = \frac{\alpha^2[(2p-1)\text{sn}(\alpha s, p)^2 - 1]}{A\text{cn}(\alpha s, p)^3}.$$

We wish to know if the derivative of the aberrancy is nonzero. All we need to do is to show that the numerator,

$$\alpha^2[(2p-1)\text{sn}(\alpha s, p)^2 - 1]$$

is nonzero. Since $\alpha^2 > 0$, we are only concerned with the second factor. By using the NSolve function in Mathematica, we see that the only solutions for the equation

$(2p-1)\mathrm{sn}(\alpha s, p)^2 - 1 = 0$ are nonreal. This fact, along with not allowing α to either equal 0 or K/α, the numerator is nonzero and the derivative as a whole is nonzero. And so, the quantity $\dot{k}/k^2$ for the two elliptic curves is also monotonic.

6.3 The Trefoil as a Spline, A Special Case

So why is the trefoil actually a good candidate for a spline? Recall that Theorem 3.2.2 gave a geometric reasoning behind Levien's claim and the aberrancy quantity $\dot{k}/k^2$ for general curves. However, the theorem is only true locally. The trefoil is actually a fascinating curve since it satisfies the conditions in the theorem globally, which is important for applications to splines. To show why the trefoil satisfies Theorem 3.2.2 globally, we will need two propositions.

First, recall that the polar coordinates of the trefoil is $r^3 = 2\cos(3\phi)$. Using ϕ as a parameter, we have

$$X(\phi) = (r\cos(\phi), r\sin(\phi)) = rU,$$

with $U = (\cos(\phi), \sin(\phi))$ and $V = (-\sin(\phi), \cos(\phi))$ being an orthonormal frame along the curve. By implicit differentiation, we get

$$\frac{dr}{d\phi} = -\frac{2\sin(3\phi)}{r^2} = -\frac{2r\sin(3\phi)}{2\cos(3\phi)} = -r\tan(3\phi).$$

This implies that

$$X'(\phi) = rV - r\tan(3\phi)U = \frac{r}{\cos(3\phi)}(\cos(3\phi)V - \sin(3\phi)U) = \frac{r}{\cos(3\phi)}T,$$

where

$$T = (-\cos(3\phi)\sin(\phi) - \sin(3\phi)\cos(\phi), \cos(3\phi)\cos(\phi) - \sin(3\phi)\sin(\phi))$$
$$= (-\sin(4\phi), \cos(4\phi)).$$

With this preliminary, we have our first proposition:

Proposition 6.3.1 *For the trefoil, the following formula holds:*

$$\theta_0 + \theta_1 = 4(\phi_0 - \phi_1),$$

where θ_0, θ_1 are the secant angles at two distinct points and ϕ_0, ϕ_1 are the polar angles of those corresponding points.

To see why this is true, suppose $P = X(\phi_0)$ and $Q = X(\phi_1)$ are two points on the leaf of the trefoil. Consider the triangle ABC formed by the x-axis and the tangent lines to the curve at P and Q. Call these tangent lines $T_0 = (-\sin(4\phi_0), \cos(4\phi_0))$ and $T_1 = (-\sin(4\phi_1), \cos(4\phi_1))$, respectively. Let ψ be the vertex angle at C, where the two tangent lines intersect. Let θ_0 and θ_1 denote the angles between the secant line PQ and the tangents at P and Q. Then $\psi = \pi - \theta_0 - \theta_1$. The base angles of the triangle at A and B can be determined to be $\measuredangle A = 4\phi_0 - \frac{\pi}{2}$ and $\measuredangle B = \frac{\pi}{2} - 4\phi_1$. See Figure 6.2. Comparing, the following formula holds:

$$\theta_0 + \theta_1 = 4(\phi_0 - \phi_1).$$

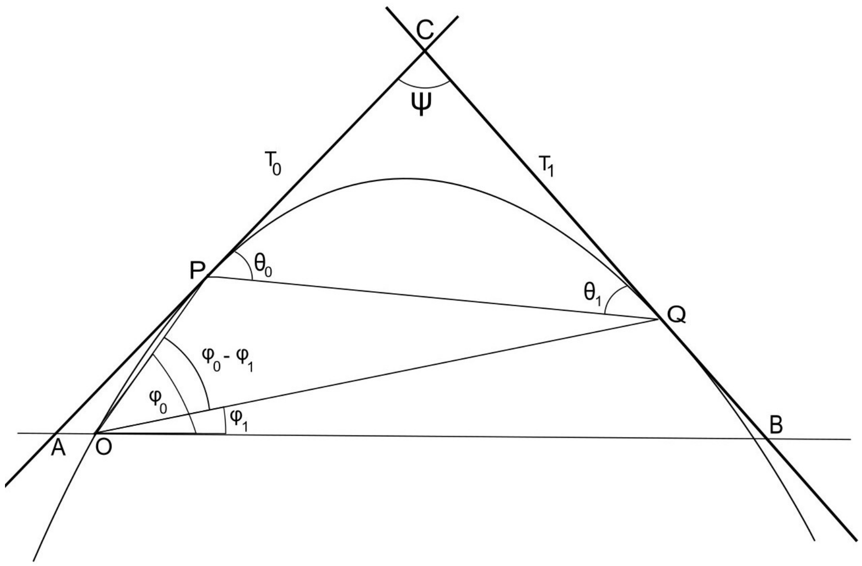

Figure 6.2: Tangents to the leaf

This formula is remarkable since it gives us a relationship between the unknown polar angles ϕ_0, ϕ_1 and the known angles between the secant lines θ_0, θ_1. The next logical step would be to find another relationship between these angles to solve for the polar angles, given any two secant angles. This relationship gives us our second proposition:

Proposition 6.3.2 *For the trefoil, the following formula holds:*

$$\cos^3(3\phi_0 - \theta_0)\cos(3\phi_0) = \cos(3\theta_0 + 2\theta_1 - 3\phi_0)\cos(3\phi_1),$$

where θ_0, θ_1 are the secant angles at two distinct points and ϕ_0, ϕ_1 are the polar angles of those corresponding points.

The proposition follows from an argument using trigonometry with information from Figure 6.2 above. With these two propositions, we have enough to state the theorem which proves that our trefoil satisfies the global result of Theorem 3.2.2.

Theorem 6.3.3 (T.A. Clark)

For the trefoil leaf, there is a one-to-one correspondence between pairs of distinct points and pairs of angles θ_0 *and* θ_1 *satisfying the constraints:* 1.) $\quad 0 < \theta_0 + \theta_1 < \dfrac{4\pi}{3}$ *and* 2.) $\quad \dfrac{1}{3} \leq \dfrac{\theta_1}{\theta_0} \leq 3.$

Proof .

We will provide a sketch of the details. There are two ways to see that this is true. The first way is the numerical approach: if the sum is constrained, then as the secant line moves around the leaf preserving the sum, one can verify that θ_0 is monotonic. The second way is the theoretical approach: the domain is simply connected and maps into the range, hitting all points on the boundary, so it is onto and it is a local homeomorphism.

∎

Pictorially, the theorem is telling us that the domain of the function that maps the pairs of distinct points and pairs of angles θ_0 and θ_1 of the trefoil is the entire rightmost leaf, where $-\dfrac{\pi}{6} < \phi_0, \phi_1 < \dfrac{\pi}{6}$. We also assume that $\phi_0 > \phi_1$ so that $\phi_0 - \phi_1 = c$, where c is a positive constant. Our domain will produce lines, all parallel to each other, all of slope 1. Using the relations $\theta_0 + \theta_1 = 4(\phi_0 - \phi_1)$ and $\phi_0 - \phi_1 = c$, we get that $\theta_1 = -\theta_0 + 4c$. So, our map sends lines of slope 1 to lines of slope -1. See Figure 6.3.

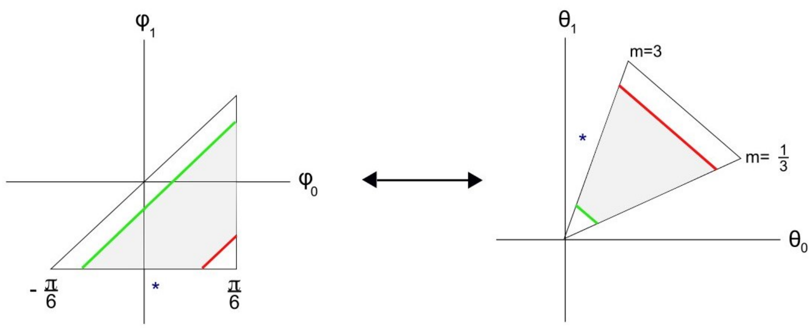

Figure 6.3: Pictorial reasoning behind Theorem 6.3.3

Now that we have a stronger statement about the trefoil, we would like to show examples of how pieces of the trefoil can be used to construct suitable splines. First, let us focus on the special instance where $\theta_0 = \theta_1$ and lie on opposite sides of the x-axis so that $\phi_1 = -\phi_0$. We will use this notion to develop a spline from a segment of the trefoil to fit a circle that circumscribes a regular polygon. For our examples, we will look at the square, the regular pentagon and the regular hexagon.

Our first example will be fitting a spline that will circumscribe a square. Let us assume that $\theta_0 = \theta_1 = \frac{\pi}{4}$. Then we know that $4(\phi_0 - \phi_1) = \theta_0 + \theta_1 = \frac{\pi}{2}$. But since the points will be symmetric along the x-axis (i.e. $\phi_1 = -\phi_0$), this implies that $\phi_0 = \frac{\pi}{16}$ and $\phi_1 = -\frac{\pi}{16}$. With this information, we can define the two points $A = (\sqrt[3]{2\cos(3\pi/16)}\cos(\pi/16), \sqrt[3]{2\cos(3\pi/16)}\sin(\pi/16))$ and $B = (\sqrt[3]{2\cos(3\pi/16)}\cos(\pi/16), -\sqrt[3]{2\cos(3\pi/16)}\sin(\pi/16))$ on the trefoil that will correspond to the angles θ_0 and θ_1 and use the maximum $C = (\sqrt[3]{2}, 0)$ as an anchor point (See Figure 6.4).

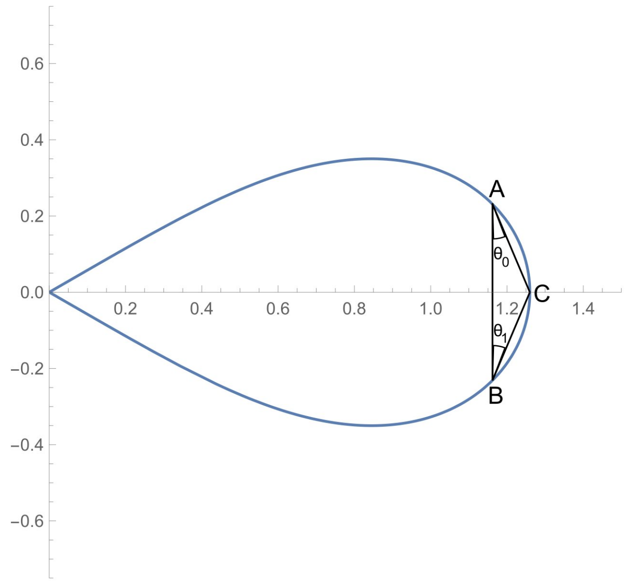

Figure 6.4: Points on the trefoil leaf

We will use the line segment between points A and B as the edge to develop the square. We find the Euclidean distance between the two points to find the length of our square, which in this case is $2(2\cos(\frac{3\pi}{16}))^{1/3}\sin(\frac{\pi}{16})$. With this knowledge, we can build the square so that the trefoil segment lines up corner to corner (or node to node, in spline terminology). These segments compose a circle around the square. The radius of the circle formed by these pieces can easily be calculated since we know the length of each side. We need to know the distance between any side and the maximum of the curve. First we pick one of the points on our initial side (in this case, I will select point A), replace the y-coordinate with 0 and find the distance between this and the maximum point C. In our case, this distance is equal to $\sqrt[3]{2}-\cos(\frac{\pi}{16})(2\cos(\frac{3\pi}{16}))^{1/3}$. And so the radius of the circle that approximates this square can be found by finding the sum of the Euclidean distance of a side and twice the length of the side to the maximum of the curve segment. In this case, the radius of our approximated circle is 0.329072. However, for regular polygons, the radius of the actual circumscribed circle is given by

$$\text{radius} = \frac{1}{2} s \csc\left(\frac{\pi}{n}\right), \text{where } s = \text{side length and } n = \text{number of sides.}$$

We can use this fact to compare the radius of the circle created by our spline to the true circle. In this case, the radius is equal is supposed to be 0.326871, which yields a percent error of 0.673294. This tells us that our spline is fairly accurate. Refer to Figure 6.5. The spline approximation is in blue while the true circle is red dotted. As we can see, the spline is a good approximation for the circumscribed circle.

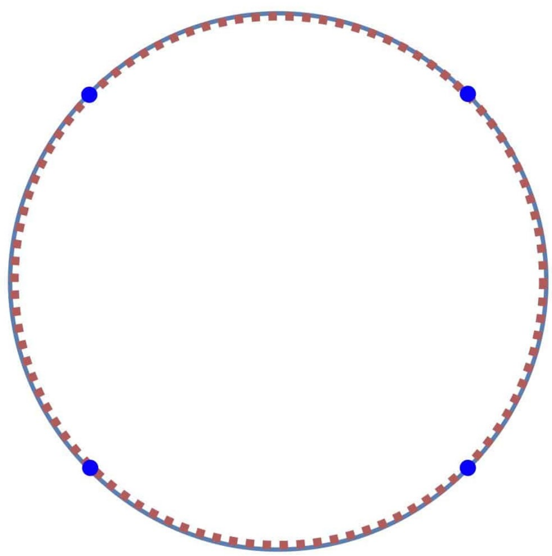

Figure 6.5: The Square with its true circumscribed circle (in red) and its trefoil spline (in blue).

We can use the same process as noted above for the pentagon and the hexagon. It should be noted that when one wants to find the radius of the approximating circle for a regular n-gon of equal sides s, calculate the height of the polygon and then add either the distance of the known side to the maximum of the trefoil (if the polygon has an odd number of sides) or twice that said distance (if the polygon has an even number of sides) where:

$$\text{height} = \begin{cases} \frac{s}{\tan(\pi/n)} & \text{if } n \text{ is even} \\ \frac{s}{2\tan(\pi/2n)} & \text{if } n \text{ is odd.} \end{cases}$$

With this, we can show that as the number of sides increase for the polygon, the better the fit becomes since the percent error gets smaller when comparing the trefoil spline radius to the true radius of the circumscribed circle. Refer to Figures 6.6 and 6.7 for a visual representation.

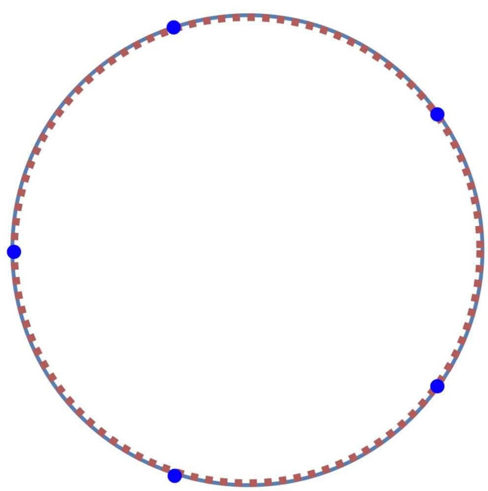

Figure 6.6: The Pentagon with its true circumscribed circle (in red) and its trefoil spline (in blue).

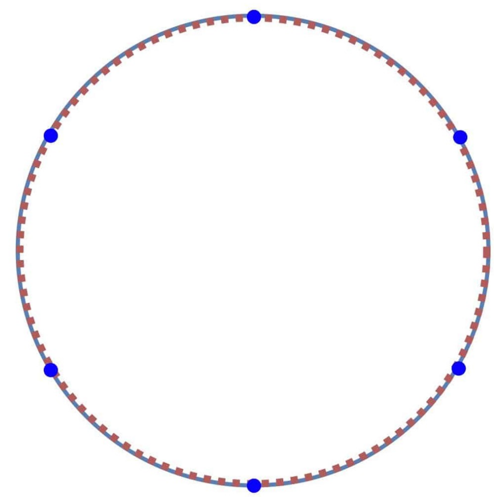

Figure 6.7: The Hexagon with its true circumscribed circle (in red) and its trefoil spline (in blue).

But we can go further in generalizing this special case. Define s as the Euclidean distance of the two points of the secant line on the trefoil where $s = 2\sqrt[3]{2}\,|\cos(3\pi/4n)^{1/3}\sin(\pi/4n)|$. We define r as the radius of the approximating circle where

$$r = \begin{cases} \sqrt[3]{2} - \sqrt[3]{2}\cos(\frac{\pi}{4n})\cos(\frac{3\pi}{4n})^{1/3} + \sqrt[3]{2}\cos(\frac{3\pi}{4n})^{1/3}\cot(\frac{\pi}{n})\sin(\frac{\pi}{4n}) & \text{if } n \text{ is even} \\ \frac{1}{2}\Big(\sqrt[3]{2} - \sqrt[3]{2}\cos(\frac{\pi}{4n})\cos(\frac{3\pi}{4n})^{1/3} + \sqrt[3]{2}\cos(\frac{3\pi}{4n})^{1/3}\cot(\frac{\pi}{2n})\sin(\frac{\pi}{4n})\Big) & \text{if } n \text{ is odd.} \end{cases}$$

We can create this table of values which compares how much better our trefoil spline approximation gets as the number of sides of the polygon increases (Refer to Table 6.1).

Table 6.1: The Approximation of the Trefoil Spline vs. the True Circle

	Square	**Pentagon**	**Hexagon**	**n-gon**
Length of side	0.462265	0.379314	0.320339	s
Radius of Trefoil Spline	0.329072	0.323089	0.320735	r
Radius of True Circle	0.326871	0.322664	0.320339	$\frac{1}{2}s\csc\left(\frac{\pi}{n}\right)$
Percent Error	0.673294	0.131571	0.123837	$\frac{200}{s}\sin(\frac{\pi}{n})\lvert s - \frac{1}{2}s\csc(\frac{\pi}{m})\rvert$

Based on the values of Table 6.1, we can see that numerically, the radius of the trefoil spline approaches a certain value. In fact, we can show that

$$\lim_{n\to\infty} r = \lim_{n\to\infty} \frac{1}{2}s\csc\left(\frac{\pi}{n}\right) = \frac{\sqrt[3]{2}}{4},$$

which is exactly what we hoped for since the radii are approaching what the true radius should be as the number of sides increase.

Chapter 7

Numerical Computation of Trefoil Splines

7.1 Numerical Calculations

In this chapter, we want to observe the fact that the trefoil satisfies Theorem 3.2.2 globally based on Theorem 6.3.1. Recall from the previous chapter that we saw a relationship between the unknown polar angles ϕ_0, ϕ_1 and the known angles between the secant lines θ_0, θ_1 of any two points of the trefoil:

$$\theta_0 + \theta_1 = 4(\phi_0 - \phi_1).$$

It is worth noting that solving for a specific choice of angles θ_0, θ_1 can be done numerically, which miraculously involves no difficult computations! Given the sum of the two angles $\theta_0 + \theta_1$ and a polar angle ϕ_0, we can find the unique ϕ_1 which tells us the measure of θ_0. This gives us the angle coordinates of the two points of the trefoil, where the resulting arc can then be explicitly generated by using the polar coordinate formula for the trefoil.

This is done by taking what we know about the trefoil and the numerical calculations from Theorem 3.2.2. The idea is that we know θ_0, which we call t, $r(t) = \sqrt[3]{2\cos(3t)}$ and the difference between ϕ_0 and ϕ_1, which we call del. Note that we allow del to vary in value. By defining $X(t) = (r\cos(t), r\sin(t))$, we can define the terms X_{10}, $X(t-\text{del})$ and $\|X_{10}\|$. This, along with the secant vector V, we can define a function $f[t, \text{del}]$ which is the dot product of the secant vector V and the normal vector at the endpoint given by t, i.e.

$$f[t, \text{del}] = \langle V, N(t) \rangle = \cos\left(\theta_0 + \frac{\pi}{2}\right) = -\sin\theta_0.$$

By taking the arcsine of both sides, we get an expression for θ_0.

Likewise, the inverse to this can be found numerically: Given the sum of the two angles $\theta_0 + \theta_1$ and the measure of angle θ_0, we can find the unique measure of ϕ_0. This is done simply finding the solution to the function

$$\arcsin(f[t, \text{del}]) + \theta_0 = 0.$$

But this is actually very easy to do since we know θ_0 and del because this reduces down to a problem of root finding, which can use either Newton's method or the Bisection method. Recall from introductory calculus that Newton's method does converge at a faster rate than the Bisection method. However, Newton does have limitations based on the initial seed value and the derivative of the function in question. for instance, Newton's method will fail if the seed value is at or near a critical point. The Bisection method requires us an interval which contains the root **and** the function needs to be continuous. While the Bisection method is slower, it has no limitations and will converge to the same answer eventually.

Mathematica codes for these problems will be provided in the appendix.

7.2 Examples of Nonlinear Splines

The good news about this numerical computation is that it provides a practical result opposed to just a theoretical one! A practical use for splines is in the development of fonts for computer word processors. This makes sense since the basis of all fonts are lines and circles, with required smoothing and adjustments for the specifics of certain letters, numerals and symbols.

One example would be the S-spline, which has three knots above the inflection, three knots below and one at the inflection. When we compare this with the circle spline back in Chapter 3, we see that our trefoil spline actually forms the letter "S" surprisingly well.

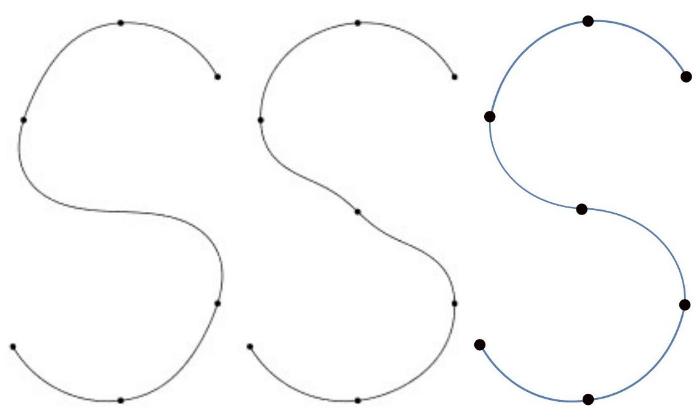

Figure 7.1: The S-spline formed by the trefoil (far right), compared to the circle spline failure.

In addition to letters, we can use pieces of the trefoil to form symbols. For instance, by using 10 knots and appropriate slices of the trefoil, we can form an ampersand which closely resembles the one on the left.

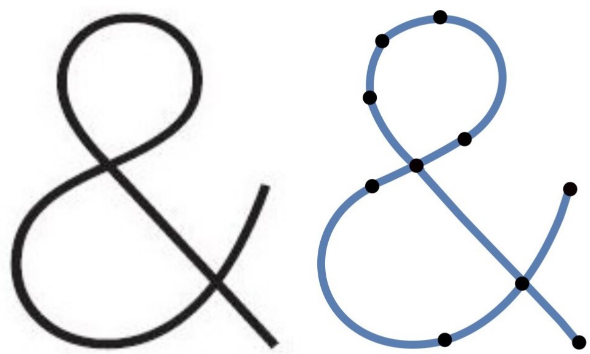

Figure 7.2: An ampersand formed by the trefoil spline (right).

With 15 knots, we can form a rough (but decent) approximation of the at symbol. Of course, with more knots, the spline will become more smooth. Regardless, even with a small number of knots, we do get a nice picture.

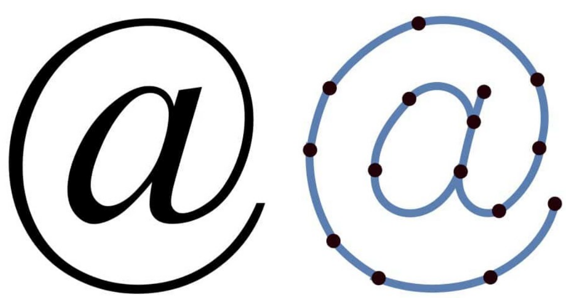

Figure 7.3: The at symbol formed by the trefoil spline (right).

Appendix A

Mathematica

In the appendix, we will provide the Mathematica code which gave us the proof to the assertions that were stated in the previous chapter. First, we provide Code *Mathematica* A.1 which answers the original problem stated in Chapter 7: Given the sum of the two angles $\theta_0 + \theta_1$ and a polar angle ϕ_0, find the measure of θ_0.

Code *Mathematica* A.2 and Code *Mathematica* A.3 provides the inverse to the problem above: Given the sum of the two angles $\theta_0 + \theta_1$ and the angle θ_0, find the measure of ϕ_0. Code *Mathematica* A.2 provides the solution to the inverse problem using the Bisection Method while Code *Mathematica* A.3 provides the solution via Newton's Method. We should note that the rate of convergence of Newton's method is typically better than the rate of convergence of the bisection method.

Code *Mathematica* A.1: Code to find θ_0, given ϕ_0

```
(*We define the polar radius r in terms of phi0, which we call t.*)

r[t_] = (2 Cos[3 t])^(1/3)

(*This is the parametrization of the trefoil in terms of polar coordinates.*)

X[t_] = {r[t] Cos[t], r[t] Sin[t]}

(*We define a value del which represents the difference between phi1 and phi0.*)

x10[t_] = X[t - del] - X[t]

len[t_] = Norm[x10[t]] // Simplify

nor[t_] = {Cos[4 t], Sin[4 t]} (*The normal vector at phi0*)

vec[t_] = 1/len[t] x10[t] (*The slope of the secant line*)

(*f[t,del] measures how the angle theta0 varies as we travel around the trefoil
leaf with fixed sum theta0+theta1=del.*)

f[t_, del_] = nor[t].vec[t]

(*We define a function Ang which produces the angle formed between the normal
vector and the secant line, given a value phi0 and del*)

Ang[t_, del_] = -ArcSin[f[t, del]]

(*The function deg is the analogue of Ang, just measured in degrees.*)

deg[t_, del_] = 180 Ang[t, del]/Pi
```

Code *Mathematica* A.2: The Bisection Method to find ϕ_0, given θ_0

```
(*We define the function b as the difference between Ang[t,del] and theta0.
Note that del and theta0 need to be defined as actual numerical values.*)

b[t_] := Ang[t, del] - (theta0)

(*The Bisection function accepts an interval and returns either the right half
or the left half of the interval, depending on whether the sign of b at the
midpoint agrees with the sign of b at the left endpoint.*)

Bisection[{lb_, ub_}] :=
If[b[lb]*b[(lb + ub)/2] > 0, {(lb + ub)/2, ub}, {lb, (lb + ub)/2}]

(*By inputting an appropriate lower bound (lower) and upper bound (upper), along
with how many iterations n, we get a sequence of estimates to m decimal places.
Note that lower, upper, n and m need to be defined as actual numerical values.*)

NestList[Bisection, {lower, upper}, n] // N[#, m] & // TableForm
```

Code *Mathematica* A.3: Newton's Method to find ϕ_0, given θ_0

```
(*We define the function n as the difference between Ang[t,del] and theta0.
Note that del and theta0 need to be defined as actual numerical values.*)

n[t_] := Ang[t, del] - (theta0)

(*The Newton function performs the Newton's method algorithm.*)

Newton[t_] := N[t - ComplexExpand[(n[t]/n'[t])]]

(*By inputting an appropriate seed value, along
with how many iterations n, we get a sequence of estimates to m decimal places.
Note that seed value, n and m need to be defined as actual numerical values.*)

NestList[Newton, seed value, n] // N[#, m] & // TableForm
```

To see this code used in practice, we will provide an example. Recall from Chapter 6 when we were calculating the necessary angles to fit a spline around the circle which would circumscribe a square. With our calculations, we saw that $\theta_0 = \theta_1 = \frac{\pi}{4}$, $\phi_0 = \frac{\pi}{16}$ and $\phi_1 = -\frac{\pi}{16}$. We wish to verify these measurements as correct. Utilizing Code *Mathematica* A.1 where $t = \phi_0 = \frac{\pi}{16}$ and del $= \phi_0 - \phi_1 = \frac{\pi}{8}$, we get the value of θ_0:

```
In[ ]:= Ang[t_, del_] = -ArcSin[f[t, del]]

In[ ]:= Ang[Pi / 16, Pi / 8]
Out[ ]= π/4
```

Now, for the inverse. Suppose we only know one of the angles formed by the secant line and tangent line of the trefoil, i.e. $\theta_0 = \frac{\pi}{4}$ and we know del $= \frac{\pi}{8}$. Then by using either the Bisection Method or Newton's Method, we get the measure of ϕ_0.

Using the Bisection Method (Code *Mathematica* A.2) with lower bound 0.1, upper bound 0.5 and 20 iterations, we get:

```
In[•]:= b[t_] := Ang[t, Pi / 8] - (Pi / 4)

In[•]:= Bisection[{lb_, ub_}] := If[b[lb] * b[(lb + ub)/2] > 0, {(lb + ub)/2, ub}, {lb, (lb + ub)/2}]

In[•]:= NestList[Bisection, {0.1, 0.5}, 20] // N[#, 20] & // TableForm

Out[•]//TableForm=
    0.1         0.5
    0.1         0.3
    0.1         0.2
    0.15        0.2
    0.175       0.2
    0.1875      0.2
    0.19375     0.2
    0.19375     0.196875
    0.195313    0.196875
    0.196094    0.196875
    0.196094    0.196484
    0.196289    0.196484
    0.196289    0.196387
    0.196338    0.196387
    0.196338    0.196362
    0.196338    0.19635
    0.196344    0.19635
    0.196347    0.19635
    0.196349    0.19635
    0.196349    0.19635
    0.196349    0.19635
```

In 20 iterations, the Bisection Method tells us that we are approaching a ϕ_0 value of 0.19635 which is approximately $\frac{\pi}{16}$! Exactly what it should be! Likewise, using Newton's Method (Code *Mathematica* A.3) with seed value 0.4 and using 20 iterations, we get:

```
In[ ]:= n[t_] := Ang[t, Pi / 8] - (Pi / 4)

In[ ]:= Newton[t_] := N[t - ComplexExpand[(n[t] / n'[t])]]

In[ ]:= NestList[Newton, 0.4, 20] // N[#, 16] & // TableForm

Out[ ]//TableForm=
        0.4
        0.261795 + 0. i
        0.19859 + 0. i
        0.19635 + 0. i
        0.19635 + 0. i
        0.19635 + 0. i
        0.19635 + 0. i
        0.19635 + 0. i
        0.19635 + 0. i
        0.19635 + 0. i
        0.19635 + 0. i
        0.19635 + 0. i
        0.19635 + 0. i
        0.19635 + 0. i
        0.19635 + 0. i
        0.19635 + 0. i
        0.19635 + 0. i
        0.19635 + 0. i
        0.19635 + 0. i
        0.19635 + 0. i
        0.19635 + 0. i
```

As we can see, in 20 iterations, Newton's Method tells us that we are approaching a ϕ_0 value of 0.19635. We are reaching a value of approximately $\frac{\pi}{16}$ at a faster rate than the Bisection Method.

BIBLIOGRAPHY

[1] Abazari, Nemat, and Yusuf Yayli. "The Classical Elastic Curves in A 3-Dimensional Indefinite-Riemannian Manifold." *Journal of Applied Sciences* **12** (2012): 1303-1307.

[2] Abramowitz, Milton, and Irene A. Stegun. "Handbook of Mathematical Functions with Formulas, Graphs, and Mathematical Tables." *US Department of Commerce.* National Bureau of Standards Applied Mathematics series 55, 1965.

[3] Andrews, Gillian, Camilla Hallinan, and Laura Sandford, eds. *The Math Book: Big Ideas Simply Explained.* Dorling Kindersley Ltd, 2019.

[4] Armitage, John Vernon, and William Frederick Eberlein. *Elliptic Functions.* Vol. 67. Cambridge University Press, 2006.

[5] Arnol'd, Vladimir Igorevich. *Mathematical Methods of Classical Mechanics.* Vol. 60. Springer Science & Business Media, 2013.

[6] Beléndez, Augusto, et al. *Exact Solution for the Nonlinear Pendulum.* Revista brasileira de ensino de física 29.4 (2007): 645-648.

[7] Birkhoff, G., H. Burchard, and D. Thomas. *Nonlinear Interpolation by Splines, Pseudosplines and Elastica*. Research Laboratories, General Motors Corporation, 1965.

[8] Birkhoff, Garrett and Carl R. De Boor. *Piecewise Polynomial Interpolation and Approximation*. 1964.

[9] Bor, Gil, Mark Levi, Ron Perline, and Sergei Tabachnikov. "Tire Tracks and Integrable Curve Evolution." *arXiv preprint arXiv:1705.06314* (2017).

[10] Brook, Alexander, Alfred M. Bruckstein, and Ron Kimmel. "On similarity-invariant fairness measures." *International Conference on Scale-Space Theories in Computer Vision*. Springer, Berlin, Heidelberg, 2005.

[11] Brunnett, Guido. *The Curvature of Plane Elastic Curves*. No. NPS-MA-93-013. Naval Postgraduate School Monterey CA Department of Mathematics, 1993.

[12] Brunnett, Guido H. "Properties of minimal-energy splines." *Curve and Surface Design*. Society for Industrial and Applied Mathematics, 1992. 3-22.

[13] Burden, R. L., and J. Douglas Faires. "Numerical Analysis 8th Edition." *Thompson Brooks/Cole* (2005).

[14] Byerley, Cameron, and Russell A. Gordon. "Measures of Aberrancy." *Real Analysis Exchange* **32.1** (2007): 233-266.

[15] Byrd, P. F., and M. D. Friedman. *Handbook of Elliptic Integrals for Scientists and Engineers*. Grundlehren der Mathematische Wissenschaften, LXVII (Springer-Verlag, Berlin, 1954) (1971).

[16] Cassel, Kevin W. *Variational Methods with Applications in Science and Engineering*. Cambridge University Press, 2013.

[17] Chapling, Richard. "Elliptic Functions." Complex Methods, University of Cambridge. Received 3 March 2016. Handout.

[18] Chapling, Richard. "Summary of Concepts in Variational Principles." Complex Methods, University of Cambridge. Received 14 October 2018. Handout.

[19] Coope, Ian D. "Curve Interpolation with Nonlinear Spiral Splines." *IMA Journal of numerical analysis* **13.3** (1993): 327-341.

[20] Cooper, Fred, Avinash Khare, and Uday Sukhatme. "Periodic solutions of nonlinear equations obtained by linear superposition." *Journal of Physics A: Mathematical and General* **35.47** (2002): 10085-10100.

[21] Cox, Steven James, et al. *Six Themes on Variation*. Vol. 26. American Mathematical Soc., 2004, pp. 1–11.

[22] Culham, J.R. "Elliptic Functions." ME755 Special Functions, University of Waterloo. Received 1 March 2004. Lecture Notes.

[23] Dalle, Derek. "Comparison of Numerical Techniques for Euclidean Curvature." *Rose-Hulman Undergraduate Mathematics Journal* **7.1** (2006): 12.

[24] Do Carmo, Manfredo P. *Differential Geometry of Curves and Surfaces: Revised and Updated Second Edition*. Courier Dover Publications, 2016.

[25] Edwards, John A. "Exact Equations of the Nonlinear Spline." *ACM Transactions on Mathematical Software (TOMS)* **18.2** (1992): 174-192.

[26] Elsgolts, Lev Ernestovich, and George Yankovsky. *Differential Equations and the Calculus of Variations*. Moscow: Mir, 1973.

[27] Faber, Richard L. *Differential Geometry and Relativity Theory: An Introduction*. Routledge, 2017.

[28] Farin, Gerald, and Dianne Hansford. *Mathematical Principles for Scientific Computing and Visualization*. AK Peters/CRC Press, 2008.

[29] Ferrández, Angel. “Some Variational Problems on Curves and Applications.” *Topics in Modern Differential Geometry.* Atlantis Press, Paris, 2017. 199-222.

[30] Finch, Steven R. Mathematical Constants. Cambridge University Press, 2003.

[31] Gelfand, Izrail Moiseevitch, and Richard A. Silverman. *Calculus of Variations*. Courier Corporation, 2000.

[32] George, Raju K. “Calculus of Variations.” Applied Mathematics, Indian Institute of Space Science and Technology. Received Fall 2017. Course Lecture Notes.

[33] Gibson, Christopher G. *Elementary Geometry of Differentiable Curves: An Undergraduate Introduction*. Cambridge University Press, 2001.

[34] Gordon, Russell A. “The Aberrancy of Plane Curves.” *The Mathematical Gazette* 89.516 (2004): 424-436.

[35] Hahn, Liang-shin, and Bernard Epstein. *Classical Complex Analysis*. Royal Society of Chemistry, 1996.

[36] Hall, Leon M. “Special Functions.” *Available in:* `http://web.mst.edu/~lmhall/SPFNS/spfns.pdf` (1995).

[37] Hermann, Martin, and Masoud Saravi. “A Brief Review of Elementary Analytical Methods for Solving Nonlinear ODEs.” *Nonlinear Ordinary Differential Equations*. Springer, New Delhi, 2016.

[38] Hicks, Noel J. *Notes on Differential Geometry*. Vol. 3. Princeton: van Nostrand, 1965.

[39] House, Donald H. "Computer Graphics." CPSC 4050/6050, Clemson University. Received 15 October 2015. Course handout.

[40] Ibrayev, Rinat, and Yan-Bin Jia. "Semidifferential Invariants for Tactile Recognition of Algebraic Curves." *The International Journal of Robotics Research* **24.11** (2005): 951-969.

[41] Itō, Kiyosi, ed. *Encyclopedic Dictionary of Mathematics.* Vol. 1. MIT press, 1993.

[42] Itō, Kiyosi, ed. *Encyclopedic Dictionary of Mathematics.* Vol. 2. MIT press, 1993.

[43] Jones, Gareth A., and David Singerman. *Complex Functions: An Algebraic and Geometric Viewpoint.* Cambridge university press, 1987.

[44] Khare, Avinash, and Avadh Saxena. "Superposition of Elliptic Functions as Solutions For a Large Number of Nonlinear Equations." *Journal of Mathematical Physics* **55.3** (2014): 032701.

[45] Khare, Avinash, and Uday Sukhatme. "Cyclic identities involving Jacobi elliptic functions." *Journal of Mathematical Physics* **43.7** (2002): 3798-3806.

[46] Komzsik, Louis. *Applied Calculus of Variations for Engineers.* CRC Press, 2018.

[47] Krantz, Steven G. *Handbook of Complex Variables.* Springer Science & Business Media, 2012.

[48] Kudryashov, Nikolai A. "Nonlinear differential equations with exact solutions expressed via the Weierstrass function." *Zeitschrift für Naturforschung A* **59.7-8** (2004): 443-454.

[49] Kühnel, Wolfgang. *Differential Geometry*. Vol. 77. American Mathematical Soc., 2015.

[50] Langer, Joel C., and David A. Singer. "Flat curves." *Mediterranean Journal of Mathematics* 14.6 (2017): 236.

[51] Langer, Joel, and David A. Singer. "Lagrangian Aspects of the Kirchhoff Elastic Rod." *SIAM review* 38.4 (1996): 605-618.

[52] Langer, J., and D. Singer. "Liouville Integrability of Geometric Variational Problems." *Commentarii Mathematici Helvetici* **69.1** (1994): 272-280.

[53] Langer, Joel C., and David A. Singer. "Subdividing the Trefoil by Origami." *Geometry* 2013 (2013).

[54] Langer, Joel, and David A. Singer. "The Total Squared Curvature of Closed Curves." *Journal of Differential Geometry* **20.1** (1984): 1-22.

[55] Langer, Joel C., and David A. Singer. "The Trefoil." *Milan Journal of Mathematics* **82.1** (2014): 161-182.

[56] Lee, Erastus H., and George E. Forsythe. "Variational Study of Nonlinear Spline Curves." *SIAM review* **15.1** (1973): 120-133.

[57] Levien, Raphael Linus. *From Spiral to Spline: Optimal Techniques in Interactive Curve Design*. Diss. UC Berkeley, 2009.

[58] Levien, Raph, and Carlo H. Séquin. "Interpolating Splines: Which is the Fairest of Them All?". *Computer-Aided Design and Applications* **6.1** (2009): 91-102.

[59] Levien, Raphael L. Patent analyzing system. US 9230350 B2, United States Patent and Trademark Office, 5 January 2016.

[60] Malcolm, Michael A. "On the Computation of Nonlinear Spline Functions." *SIAM Journal on Numerical Analysis* **14.2** (1977): 254-282.

[61] Menger, Karl. "What is Calculus of Variations and What are its Applications?." *The Scientific Monthly* **45.3** (1937): 250-253.

[62] Mladenov, Ivaïlo M., and Mariana Hadzhilazova. *The Many Faces of Elastica*. Cham: Springer, 2017.

[63] Moreton, Henry Packard. *Minimum Curvature Variation Curves, Networks, and Surfaces for Fair Free-Form Shape Design*. Diss. University of California, Berkeley, 1992.

[64] Moreton, Henry P., and Carlo H. Séquin. "Minimum Variation Curves and Surfaces for Computer-Aided Geometric Design." *Designing Fair Curves and Surfaces: Shape Quality in Geometric Modeling and Computer-Aided Design*. Society for Industrial and Applied Mathematics, 1994. 123-159.

[65] Moreton, Henry P., and Carlo H. Séquin. "Scale-Invariant Minimum-Cost Curves: Fair and Robust Design Implements." *Computer Graphics Forum*. Vol. 12. No. 3. Edinburgh, UK: Blackwell Science Ltd, 1993.

[66] *NIST Digital Library of Mathematical Functions*. `http://dlmf.nist.gov/`, Release 1.0.23 of 2019-06-15. F. W. J. Olver, A. B. Olde Daalhuis, D. W. Lozier, B. I. Schneider, R. F. Boisvert, C. W. Clark, B. R. Miller, and B. V. Saunders, eds.

[67] Özkan, Gözde and Ahmet Yücesan. "Relaxed Elastic Line in a Riemannian Manifold." (2014).

[68] Pastras, Georgios. "Four Lectures on Weierstrass Elliptic Function and Applications in Classical and Quantum Mechanics." 2017. arXiv:1706.07371

[69] Prenter, Paddy M. *Splines and Variational Methods*. Courier Corporation, 2008.

[70] Sapidis, Nickolas S., and George D. Koras. "Visualization of Curvature Plots and Evaluation of Fairness: An Analysis of the Effect of 'Scaling'." *Computer Aided Geometric Design* **14.4** (1997): 299-311.

[71] Schot, Steven H. "Aberrancy: Geometry of the Third Derivative." *Mathematics Magazine* **51.5** (1978): 259-275.

[72] Schwalm, William A. *Lectures on Selected Topics in Mathematical Physics: Elliptic Functions and Elliptic Integrals*. Morgan & Claypool Publishers, 2015.

[73] Séquin, Carlo H., P-Y. Chang, and Henry P. Moreton. "Scale-Invariant Functional for smooth curves and surfaces." *Geometric Modelling*. Springer, Vienna, 1995. 303-321.

[74] Singer, David A. "Curves Whose Curvature Depends on Distance from the Origin." *The American mathematical monthly* **106.9** (1999): 835-841.

[75] Singer, David A. "Lectures on Elastic Curves and Rods." *AIP Conference Proceedings*. Vol. 1002. No. 1. AIP, 2008.

[76] Skullerud, Jon-Ivar, and Brian Dolan. "Classical Mechanics." MP350, Maynooth University. Received Spring 2012. Lecture Notes.

[77] Solomon, Justin H. "Isometry Invariance and Spectral Techniques." CS 468, Stanford University. Received Spring 2013. Course handout.

[78] Spivak, Michael. *Physics for Mathematicians: Mechanics I*. Publish or Perish, 2010.

[79] Temme, Nico M. *Special Functions: An Introduction to the Classical Functions of Mathematical Physics*. John Wiley & Sons, 2011.

[80] Wang, Kai. "A Study of Cubic Spline Interpolation." *InSight: Rivier Academic Journal* **9.2** (2013).

[81] Washington, Lawrence C. *Elliptic Curves: Number Theory and Cryptography*. Chapman and Hall/CRC, 2003.

[82] Wikipedia contributors. "Dixon's elliptic functions." *Wikipedia, The Free Encyclopedia*. Wikipedia, The Free Encyclopedia, 14 Feb. 2019. Web. 9 Sep. 2019.

[83] Zhu, Yongchang. "Elliptic Functions and Theta Functions." Math 4999, The Hong Kong University of Science and Technology. Received 22 Nov. 2016. Course lecture notes.